

See discussions, stats, and author profiles for this publication at: <https://www.researchgate.net/publication/305417274>

Presalt stratigraphy and depositional systems in the Kwanza Basin, offshore Angola

Article in AAPG Bulletin · July 2016

DOI: 10.1306/02111615216

CITATIONS
83

READS
4,824

6 authors, including:



Arthur Saller

Kosmos

75 PUBLICATIONS 2,110 CITATIONS

[SEE PROFILE](#)

Some of the authors of this publication are also working on these related projects:



Permian Basin [View project](#)

Presalt stratigraphy and depositional systems in the Kwanza Basin, offshore Angola

Arthur Saller, Shawn Rushton, Lino Buambua, Kerry Inman, Ross McNeil, and J. A. D. (Tony) Dickson

ABSTRACT

The Lower Cretaceous presalt section in the Kwanza Basin contains an excellent petroleum system that includes “synrift” strata (Barremian) overlain by a “sag” interval (Aptian) and capped by the Loeme Salt. The upper synrift is generally limestone with widespread mollusk packstones and grainstones (coquinas) deposited in a fresh-to-moderately saline (alkaline) lake. The sag interval is characterized by carbonate platforms and silica-rich isolated buildups formed in highly evaporated, highly alkaline lakes. Shrubby (dendritic), microbially influenced boundstones and intraclast-spherulite grainstones accumulated in shallow water on platform tops. Microbial cherts were deposited as organic buildups on large, isolated structural highs basinward (west) of platforms, and they apparently formed at low temperatures in very alkaline lake water. Shrubby boundstones and microbial cherts have vuggy pores that are primary and result in high permeability. Wackestones and packstones with calcitic grains (mainly spherulites) in dolomite or argillaceous dolomite were deposited in slightly deeper, low-energy sag environments. In addition, clays (especially stevensite) precipitated out of the silica-rich, highly alkaline lake waters. During sag deposition, calcite precipitated on the shallow lake floor with morphologies that ranged from spherulites to shrubs and included a continuum of intermediate forms. Spherulites probably precipitated just below the sediment-water interface. Spherulites and shrubby calcites are commonly recrystallized. Spherulites floating in stevensite probably formed in deeper lacustrine environments. Organic-rich mudstones were deposited in even deeper lacustrine environments in synrift and sag intervals, and they are likely the source of most hydrocarbons in this system. These interpretations are supported by seismic, core, petrographic, and stable isotope data.

AUTHORS

ARTHUR SALLER ~ Cobalt International Energy, 920 Memorial City Way, Suite 100, Houston, Texas 77024; arthur.saller@cobaltintl.com

Art Saller is a carbonate sedimentologist and stratigrapher for Cobalt International Energy in Houston. He attended the University of Kansas (B.S., 1977), Stanford University (M.S., 1980), and Louisiana State University (Ph.D., 1984). Art has had the pleasure of working for Cities Service Oil and Gas in Tulsa (1984–1986); Unocal in Brea, California and Houston (1986–2005); and Chevron in Houston (2005–2012).

SHAWN RUSHTON ~ Cobalt International Energy, 920 Memorial City Way, Suite 100, Houston, Texas 77024; shawn.rushton@cobaltintl.com

Shawn Rushton is an exploration geophysicist with over 16 years of experience in the industry. He has worked for small- and medium-sized oil and gas companies on projects all over the world. He received a B.Sc. degree (1998) in geology/geophysics and an M.Sc. degree (2000) in geophysics from the University of Calgary. He currently works for Cobalt International Energy Inc. in exploration.

LINO BUAMBUA ~ Sonangol EP, Edificio Sede, Rua Rainha Ginga 29-36, Luanda, Angola; lino.buambua@sonangol.co.ao

Lino Buambua is an exploration geologist with over 15 years of experience in the petroleum industry currently working for Sonangol in West Africa, Europe, and the United States. He received a B.Sc. degree (1993) in geology from Rio de Janeiro Federal University and an M.Sc. in geoscience (1996) from the University of Campinas (Unicamp–Brazil).

KERRY INMAN ~ Cobalt International Energy, 920 Memorial City Way, Suite 100, Houston, Texas 77024; Kerry.Inman@cobaltintl.com

Kerry Inman is an exploration geologist for Cobalt International Energy in Houston, where she has worked for the past 10 years. Prior to joining Cobalt, she worked as an independent consultant and for Sohio/BP, primarily focused on regional analysis and prospect generation.

Copyright ©2016. The American Association of Petroleum Geologists. All rights reserved.

Manuscript received November 2, 2015; provisional acceptance January 12, 2016; revised manuscript received January 24, 2016; final acceptance February 11, 2016.

DOI:10.1306/02111615216

She received a B.A. degree in geology from Colgate University and an M.S. from the University of Arizona.

Ross McNEIL ~ *Cobalt International Energy, 920 Memorial City Way, Suite 100, Houston, Texas 77024; Ross.McNeil@cobaltintl.com*

Ross McNeil is an exploration geophysicist with over 20 years of experience in domestic and international exploration. He received a B.S. degree in geophysics from the University of California at Santa Barbara and an M.S. degree in geophysics from the University of Utah. He currently works for Cobalt International Energy.

J. A. D. (TONY) DICKSON ~ *Department of Earth Science, Downing Street, Cambridge University, Cambridge CB2 3EQ, United Kingdom; jadd1@esc.cam.ac.uk*

Tony Dickson has B.Sc. and Ph.D. degrees in geology (London University, England); has taught at Cardiff, Nottingham, and Cambridge Universities; has given many industry courses; and has consulted on carbonate diagenesis (Central Basin Platform, Texas; Tarim Basin, China; Tengiz, Kazakhstan; Wafra, Neutral Zone; and Kwanza Basin, Angola). He is a recipient of the Wollaston Fund (Geological Society, London) and the Pettijohn Medal (SEPM).

ACKNOWLEDGMENTS

We thank Sonangol EP, BP, Sonangol P&P, and Cobalt International Energy for permission to publish this manuscript. We received insight and help from many colleagues at Cobalt, including Chris Olson, Tim Nicholson, John Shinol, Shawn Mulcahy, Keith Jantz, Ryan Murphy, Truitt Smith, Jim Farnsworth, James Painter, April Parsons, Ed Cazier, Connie Bargas, Chris Davin, Paul Langlois, Steve Mondziel, Lynne Hackedorn, Jennifer Lewis, Richard Redhead, Chris Calnan, Mike Cleveland, Owen BeMent, Mugabe Goncalves, Olimpia Custodio, Yolanda Silva, Jim Geary, Renee Porter, Kim Mettes, Tony Gonnell, and António Vieira. Several other people provided important support for this study, including Kate Giles, Greg Wahlman, Reed Glasman, Nicola Adams, Domingos Cunha, Francisca B. C. Lemos V. D. da Silva, Alípio Lopes, Hercínia

INTRODUCTION

Both sides of the South Atlantic contain major petroleum provinces with oil in reservoirs extending from Lower Cretaceous carbonates to Neogene sandstones. The basin history included widespread salt deposition in the upper Aptian. Strata deposited before salt deposition are referred to as “presalt.” Substantial amounts of oil have been produced from presalt strata for several decades in Brazil and West Africa (Guardado et al., 1990; McHargue, 1990; Dale et al., 1992). Recent large discoveries in Brazil (Carminatti et al., 2008) have made the presalt play very important globally. The presalt play in Angola was rejuvenated by recent discoveries in the Kwanza Basin (Greenhalgh et al., 2012; Cazier et al., 2014). The purpose of this paper is to present data and interpretations on presalt stratigraphy and depositional facies in the Kwanza Basin, offshore Angola, which appear similar to the presalt systems in Brazil. For confidentiality reasons, we avoid giving well names and depths in this paper.

GENERAL SETTING

South America started to separate from Africa in the Early Cretaceous, with rifting and sea floor spreading beginning in the south and migrating to the north (Figure 1; Fairhead and Wilson, 2005; Davison, 2007). Rifting created a series of horsts, grabens, and half grabens from Gabon to south Angola (Torsvik et al., 2009). As rifting spread from south to north, basin development progressed from many smaller grabens and lakes (“synrift”) to regional subsidence creating widespread lacustrine “sag” deposits (Carminatti et al., 2008; Quirk et al., 2013). In offshore Angola and Brazil, the entire presalt section of siliciclastic and carbonate strata is interpreted as deposition in a series of lakes and associated terrestrial environments ranging in age from Hauterivian to lower upper Aptian (133–117 Ma; Figure 2; Quirk et al., 2013).

Early rift deposition was dominated by siliciclastics (siliceous mudstones, sandstones, conglomerates). However, during the later stages of rifting (Barremian), areas that include current offshore Angola and southern Brazil had substantial lacustrine carbonate deposition (Guardado et al., 1990; Dale et al., 1992), whereas sandstones were deposited in the northern part of the rift (Gabon). In both areas, the axes of deeper grabens were dominated by organic-rich mudstone, which would become a prolific oil-prone source rock upon deeper burial (Schoellkopf and Patterson, 2000).

Biostratigraphy, based mainly on ostracods, indicates that much of the synrift section, including Toca carbonates in northern Angola, is Barremian in age (ostracod stages AS6–AS10 of Guardado et al., 1990; McHargue, 1990; Bate, 1999). Our biostratigraphy

and seismic stratigraphy are in accordance with those previous interpretations. Widespread faulting and graben creation greatly slowed or stopped in our study area near the end of the Barremian (AS10), based on seismically defined faulting and biostratigraphy.

The Toca and adjacent presalt strata in northern Angola (Cabinda area) have been interpreted as lacustrine in many studies (McHargue, 1990; Dale et al., 1992; Bate, 1999; Harris, 2000; Poropat and Colin, 2012; Quirk et al., 2013). Previous interpretations of a lacustrine environment for presalt carbonates were based on numerous features: (1) paleogeographic maps of offshore Angola, Congo, and Gabon show that those areas were separated from the open Atlantic Ocean by the Walvis Ridge prior to the middle Aptian (Torsvik et al., 2009, and others); (2) the presalt interval including Toca carbonate lacks in-place marine fossils (Poropat and Colin, 2012); (3) presalt strata contain ostracods indicative of a nonmarine lacustrine environment (Bate, 1999; Poropat and Colin, 2012); and (4) stevensite, a mineral indicative of deposition in alkaline lakes (Cerling, 1994; Wright, 2012), is present in the Toca and Kwanza Basin presalt intervals (Poropat and Colin, 2012; Wright, 2012).

Prior to deposition of the Loeme Salt, intense rifting and associated faulting stopped, and the basin went through a period of sag deposition. In more landward parts of the basin, sag deposition was minimal or dominated by siliciclastics (Chela sandstones and equivalents) (Quirk et al., 2013). Broad subsidence during deposition of the sag interval (early to middle Aptian) allowed accumulation of carbonates on structural highs currently in deep-water parts of offshore Angola and Brazil (Carminatti et al., 2008).

Aptian regional subsidence allowed seawater to flood into the Kwanza and Congo Basins from the south. This initially caused widespread salt deposition during the late Aptian, followed by restricted marine carbonates and evaporites, and then open marine deposition (latest Aptian to early Albian). Depositional environments became progressively deeper marine during the Late Cretaceous and early Paleogene (Torsvik et al., 2009).

METHODS

Rock material used in this study came from conventional cores, rotary sidewall cores, and well cuttings. All were processed with routine protocols. Materials for thin sections were impregnated with blue plastic, and thin sections were stained with a solution containing Alizarin Red S and potassium ferricyanide as per Dickson (1966).

Carbon ($\delta^{13}\text{C}$) and oxygen ($\delta^{18}\text{O}$) isotope analyses of carbonates were run on approximately 250 μg samples of dried, homogenized carbonate sealed with silicone rubber septa and a

Cordeiro Gomes Ferreira, Paulo Marinho, Mário Dias, and Mário Caetano. Thanks are also due to the following people for isotope analyses: James Rolfe of The Godwin Laboratory for Palaeoclimate Research, Department of Earth Sciences, University of Cambridge; Adrian Boyce, The Scottish Universities Environmental Research Centre; and John Craven, Ion Microprobe Facility, School of Geosciences, The University of Edinburgh. We are grateful to Schlumberger Multiclient and CGG Multiclient for giving us permission to use their seismic profiles. We also thank AAPG reviewers Toni Simo and Gabor Tari as well as subeditor Claudio Bartolini for help in publishing this article.

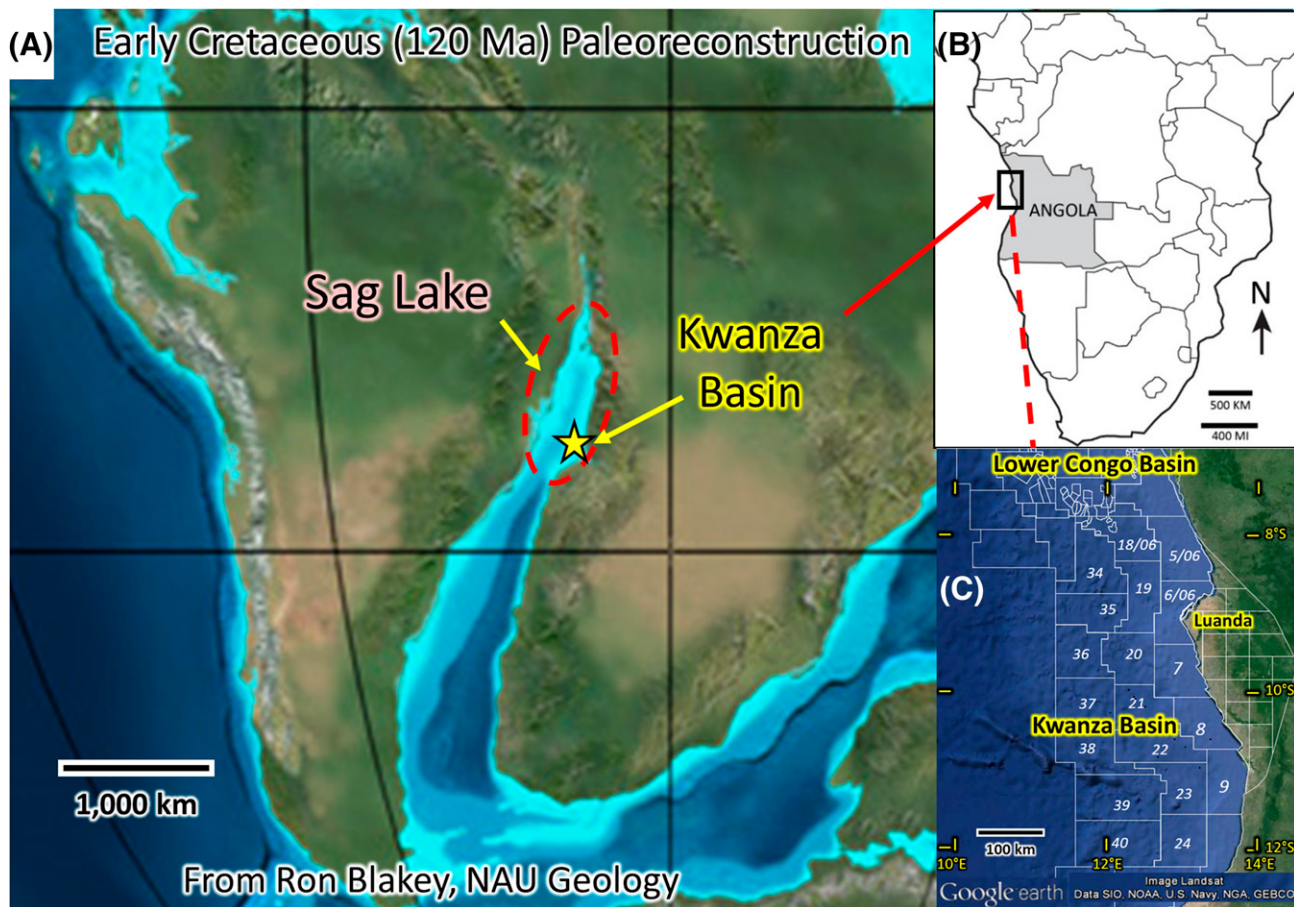


Figure 1. (A) Paleoreconstruction showing the relative locations of South America (left) and Africa (right) at approximately 120 Ma (Early Cretaceous). (B) Location of our study area, Kwanza Basin, offshore Angola. (C) Map of concession areas, offshore Angola, superimposed on Google Earth image. Cobalt International Energy operated Blocks 9, 20, and 21. Material shown in this paper is from those blocks. GEBCO = General Bathymetric Chart of the Oceans; NAU = Northern Arizona University; NGA = National Geospatial-Intelligence Agency; NOAA = National Oceanic and Atmospheric Administration, Department of Commerce; SIO = Scripps Institution of Oceanography.

screw cap in screw-cap vials. The samples were analyzed using a Thermo Gas Bench preparation system attached to a Thermo MAT 253 mass spectrometer in continuous flow mode. The results are reported with reference to the international standard, Vienna PeeDee belemnite, and the precision is better than $\pm 0.08\text{\textperthousand}$ for $\delta^{13}\text{C}$ and $\pm 0.10\text{\textperthousand}$ for $\delta^{18}\text{O}$.

Bulk rock $\delta^{18}\text{O}$ analyses were run on silica samples using laser fluorination. Ground samples were washed in a 15% hydrogen chloride (HCl) solution, rinsed, reacted with ClF_3 to release oxygen that was converted to carbon dioxide (CO_2) by reaction with hot graphite, and analyzed by a VG Optima mass spectrometer. Reproducibility was better than $\pm 0.3\text{\textperthousand}$ (one standard deviation).

The $\delta^{18}\text{O}$ analyses were also run on silica samples using the Cameca IMS-4f ion microprobe. A focused primary beam of $^{133}\text{Cs}^+$ ions was accelerated onto gold-

coated, polished thin sections. Negative, high-energy secondary ions ($^{18}\text{O}^-$ and $^{16}\text{O}^-$) were accelerated and focused into a mass spectrometer where the isotopes were magnetically separated and counted with an electron multiplier. Analytical precision using the secondary ion mass spectrometry technique was $\pm 1.0\text{\textperthousand}$.

MINERALS

In addition to siliciclastic detritus transported into depocenters in the Kwanza Basin, presalt strata contain various minerals precipitated from ions dissolved in the lake water. The main minerals precipitated in the presalt of the Kwanza Basin are listed in Table 1.

Calcium carbonate can be precipitated as calcite or aragonite. Aragonite is very common in modern

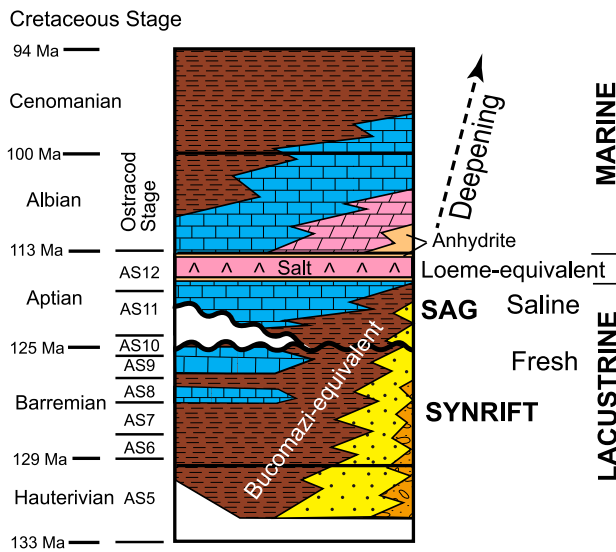


Figure 2. Schematic Cretaceous stratigraphy for the Kwanza Basin. Ages for geological stage boundaries are from Cohen et al. (2013). Approximate locations of ostracod stages are from Poropat and Colin (2012).

shallow marine environments. Aragonite is “metastable” relative to calcite, and hence it has generally been transformed to calcite (“neomorphosed” or otherwise replaced) in most pre-Pleistocene carbonates throughout the world. Aragonite inclusions or relicts may remain in calcites neomorphosed from aragonite. Aragonite is not present in the existing presalt section. Calcite occurs in many forms, including mollusk shells (many of which recrystallized from aragonite), dendritic (shrubby) growths,

spherulites (small, round grains with radiating crystals), ostracod shells, intraclasts, and micrite. All of these forms are compatible with deposition in a lake. No open marine fossils (echinoderms, foraminifera, etc.) have been found in the presalt section in this study. Calcite also occurs as an early and late cement.

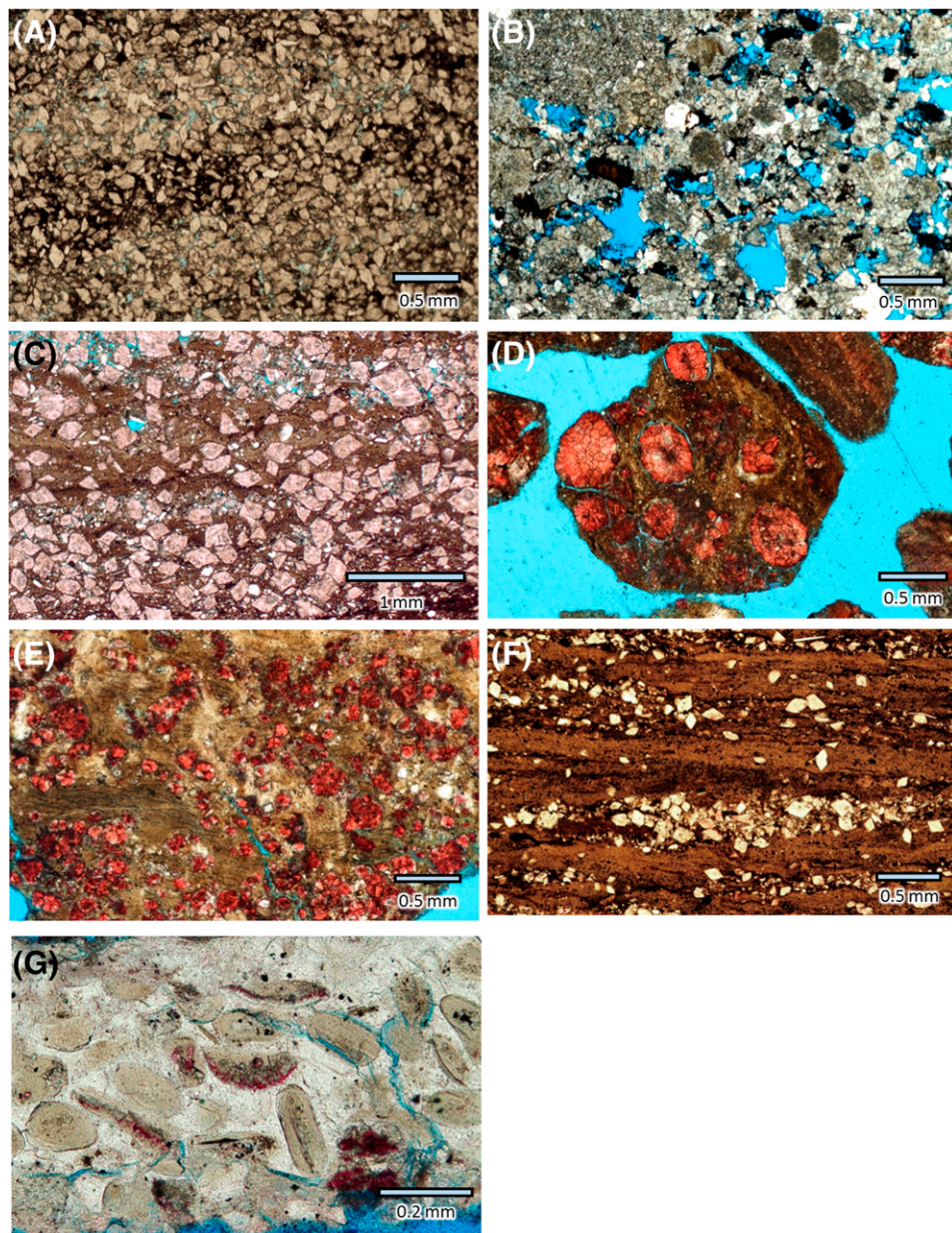
Dolomite is a common mineral in the presalt of the Kwanza Basin. Dolomite (Figure 3A, B) occurs as (1) a primary precipitate with no apparent precursor, (2) a diagenetic replacement of a precursor carbonate, and (3) a pore-filling cement. In many cases, it is difficult to prove that a specific occurrence of dolomite precipitated directly out of a lake, but in some intervals, dolomite (“crystalline dolomite”) occurs as evenly spaced crystals with no apparent precursor (Figure 3A) and hence could be primary. Other dolomites are clearly replacive (Figure 3B). Microcrystalline dolomite that occurs in very organic-rich strata could also have precipitated directly out of lake water. Euhedral, delicately zoned dolomite crystals occurring in stevensite-rich layers are also likely primary, being precipitated directly out of the lake waters. In some intervals, dolomite crystals have been replaced by calcite (Figure 3C; “dedolomite”).

Chert is variable in its occurrence but is locally abundant. Chert occurs as microbial boundstones that apparently precipitated from lake water, often on topographic highs. Thin chert beds are also present in more micritic intervals in sag platform deposits. Chert is also observed as a replacive mineral, especially in the synrift interval. Chalcedony

Table 1. Minerals, Grains, and Other Structures Precipitated from Lake Waters

Mineral	Grains and Other Precipitated Material
Calcite and aragonite: CaCO_3	Mollusk shells Spherulites Shrubs Ostracods Micrite
Dolomite: $\text{CaMg}(\text{CO}_3)_2$	Layered dolomite crystals Microbialites
Chert: SiO_2	Microbial boundstone Chalcedony (syndepositional cement)
Stevensite: $(\text{Ca}_{0.5}, \text{Na})_{0.33}(\text{Mg}, \text{Fe}^{2+})_3\text{Si}_4\text{O}_{10}(\text{OH})_2 \cdot n(\text{H}_2\text{O})$	Clay mud
Saponite: $\text{Ca}_{0.1}\text{Na}_{0.1}\text{Mg}_{2.25}\text{Fe}^{2+}_{0.75}\text{Si}_3\text{AlO}_{10}(\text{OH})_2 \cdot 4(\text{H}_2\text{O})$	Peloids Ooids

Figure 3. Thin-section photomicrographs from Kwanza Basin presalt strata. Thin sections were stained with Alizarin Red S. Calcite appears red, and porosity is blue. (A) Dolomite with euhedral-to-subhedral crystals that may have precipitated directly out of lake waters (primary dolomite). Clay (dark brown) is present between dolomite crystals. (B) Dolomite that has replaced originally calcitic grains. (C) Calcite in shapes of dolomite rhombs (pink) indicating that dolomite initially precipitated with the stevensite (brown) and then was calcitized, probably in the shallow subsurface, because of changing magnesium/calcium in the lake water ("dedolomite"). (D) Spherulites (red) in stevensite clay (brown). (E) Small spherulites (red) in stevensite clay (brown). (F) Dolomite rhombs (light brown to white) in stevensite clay (medium to dark brown). (G) Stevensite oolitic coatings and grains (light brown) with intergranular quartz cement (white).



and quartz cements are locally common in cherty microbial boundstones.

Under certain geochemical conditions (very high alkalinity), clay can precipitate from lake water (Wright and Barnett, 2015). These clay minerals include stevensite, saponite (a member of the stevensite family), and sepiolite. Stevensite has been repeatedly identified in the presalt of the Kwanza Basin. Stevensite is observed (1) precipitated in beds with dolomite or calcitic spherulites (Figure 3D-F), (2) precipitated in isolated layers, (3) as oolitic coatings on grains in the lower part of the synrift (Figure 3G),

and (4) in trace amounts in other carbonate facies, including shrubby microbialites.

SAG DEPOSITIONAL FACIES

The presalt of the Kwanza Basin contains many depositional facies. Many facies are confined to the sag (Aptian), whereas other facies are confined to the synrift (Barremian; Figure 4). Several siliciclastic-rich or mud-rich facies occur in both the synrift and sag intervals. Some of the presalt facies exhibit

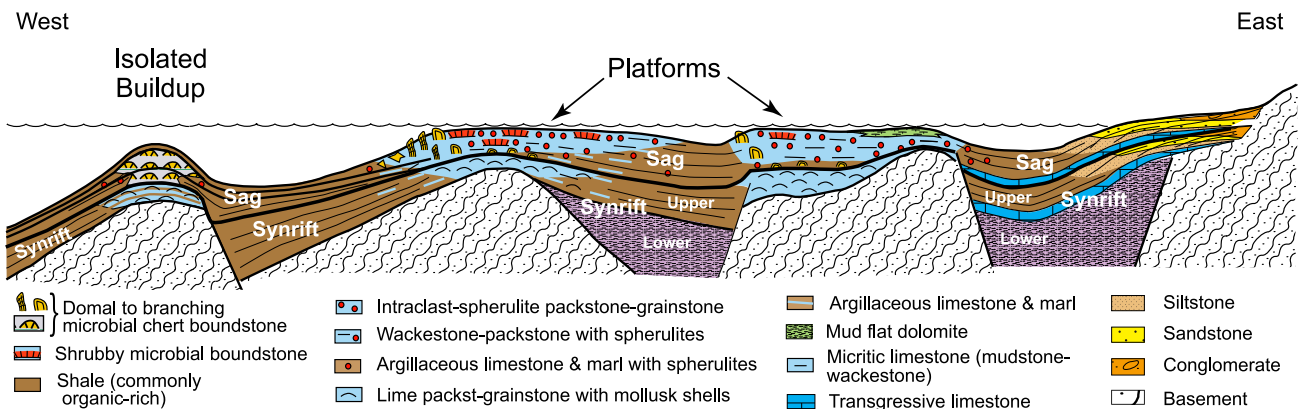


Figure 4. Schematic stratigraphic model for presalt in the Kwanza Basin. The top surface shows a depositional model (facies and bathymetry) for the upper sag. packst = packstone.

characteristics similar to those that accumulate in fluvial and marine environments, whereas others are distinctly different.

In general, mollusks are absent in the sag interval. Ostracods are also absent in most of the sag interval, but they do occur in a few beds. Several different forms of microbialites are present in the sag. Laminae with transported grains or mud deposited (trapped) on microbial mats are extremely rare. Microbial boundstone textures are dominated by carbonate or silica that was apparently precipitated in or on the boundstone structure, giving morphologies similar to modern marine coral and coralline algal reefs. Other types of grains in the sag include spherulites, intraclasts, and peloids. The main carbonate and chert facies identified in the central-to-western parts of Kwanza Basin in the sag interval are described below.

Shrubby Boundstone

The shrubby boundstone facies (morphologic description similar to Chafetz and Guidry, 1999; Wright and Barnett, 2015) consists of upward bifurcating, dendritic carbonate “branches” that are commonly 1–5 mm (0.04–0.20 in.) across and occur in layers 1 mm (0.04 in.) to 70 cm (28 in.) thick (Figures 5 and 6). Layers of shrub-like growths (simplified to “shrubs”) are interrupted by mud or grain-rich laminations and layers. Elongate primary pores (vugs) are common between branches. Shrub branches generally consist of radiating bundles of fibrous-to-prismatic calcite crystals. Within a shrub branch, upward-oriented bundles of radiating fibrous crystals have

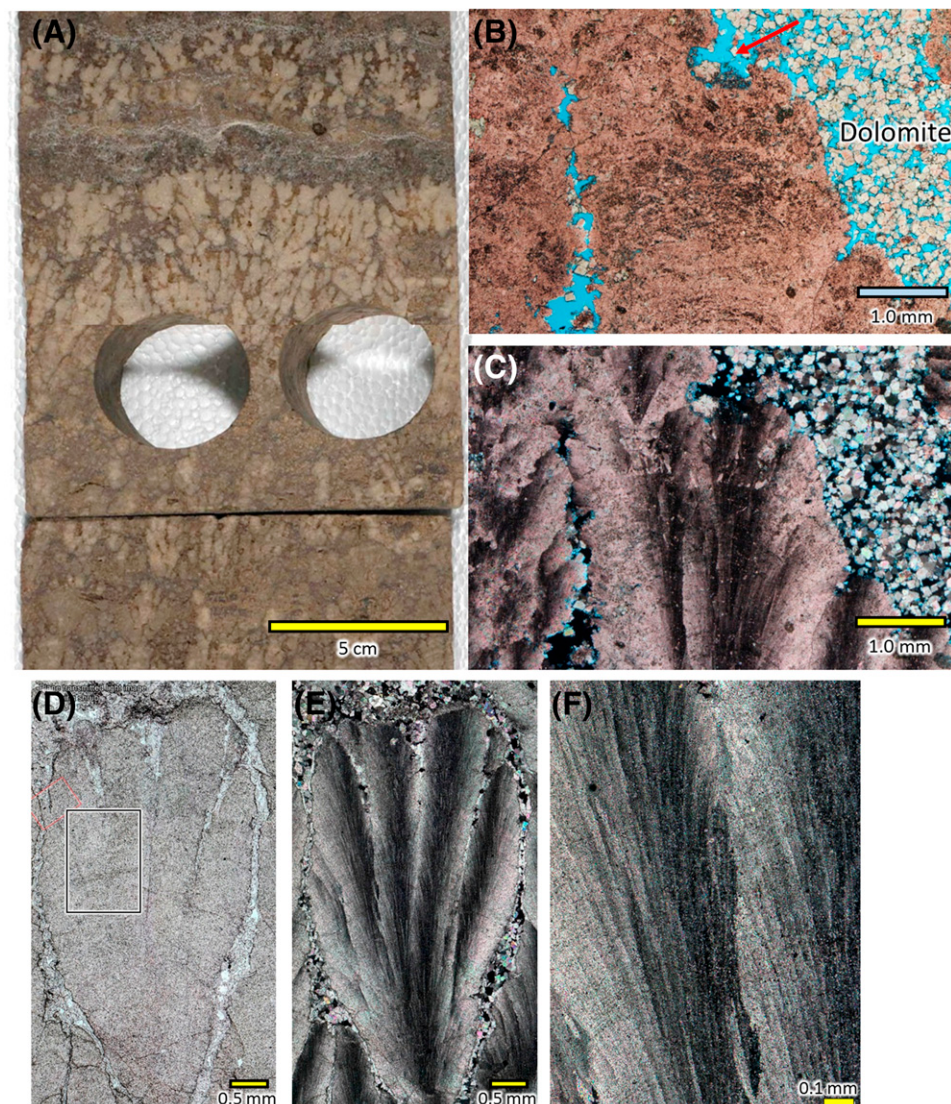
clear growth interference; however, the fibrous, upward-oriented bundles abruptly end at the edge of a branch, leaving open vugs between shrubby growths (Figures 5 and 6). The shrubs appear to have grown upward and created positive relief.

Many shrubs have dark, irregular laminations and erosional embayments (Figure 7A–D). Some shrubs show micritization at the terminations of fibrous crystal growths. Some of the best-preserved shrubs are microporous. The irregularly shaped micropores are crudely arranged along concentric and radial patterns and are secondary (Figure 7E). Small, irregularly shaped dolomite crystals are present within most shrubs. Cores of extensively altered shrubs had macropores that were sometimes filled with large zoned dolomite crystals and are sometimes still open. Shrubby calcite is pseudopleochroic in thin section because of fluid-filled pores (inclusions). Shrub calcites contain, on average, 3000 ppm strontium. A spotted cathodoluminescent pattern (Figure 7F) indicates that even the best-preserved shrubs have been recrystallized. Some shrubs have been dolomitized.

Dolomite crystals are common in pores adjacent to shrubby growths (Figures 5B; 6E; 7A–D). The dolomite crystals are generally euhedral to subhedral, show multiple zones in cathodoluminescence, and range in abundance from absent to filling almost all pore space between shrubby growths. Petrographically, they grew after the adjacent shrubby calcite; however, the dolomites appear to be diagenetically early.

This facies has been interpreted to form in a very saline-to-alkaline lacustrine environment in the pre-salt of Brazil (Wright and Barnett, 2015). A general lack of calcareous biota (mollusks, ostracods) suggests

Figure 5. Core photograph (A) and photomicrographs (B–F) of shrubby boundstones. (A) Shrubby growth (light brown) with dendritic upward branches alternating with grainstone intervals (dark layers). (B) Calcitic shrub showing upward growth, with dark inclusions and an embayment (arrow) probably related to microbial erosion. Stained with Alizarin Red S. Calcite is red. Porosity is blue. (C) Cross-polarized view of (B). Fibrous calcite crystals with radiating extinction and vertical crystal orientations. (D) Shrubby growth. (E) Cross-polarized view of (D). Bundles of fibrous calcite crystals with radiating extinction and crystal orientations. (F) Close up of black rectangle in (D). Cross-polarized view with bundles of fibrous calcite crystals with radiating extinction and crystal orientations.



deposition of this facies in a stressed (very saline to alkaline) environment (Van Damme and Gautier, 2013). Presalt shrubs have been suggested to be microbial (inferred from statements in Carminatti et al., 2008) and abiotic by others (Dorobek et al., 2012; Wright and Barnett, 2015). These dendritic structures are similar to biotic reefal organisms growing toward light and appear to be creating positive structures similar to reefs. Dark, organic laminations and erosional embayments support microbial influence, but there are bundles of fibrous calcite without organic laminations or embayments that could be abiotic. The lack of sediment and early fibrous crystals in voids between branches suggests a barrier or baffle to water flow between the top of the shrub and open vugs below. A microbial mat or

biofilm at the top of the shrubby growth might not have been the cause of the calcareous precipitate, but it could have prevented sediment from falling between the shrub branches and might have stopped supersaturated waters from percolating down and precipitating cements between the branches.

No evidence of an original aragonite precursor has been identified in the shrubs. In marine carbonates, neomorphic calcite replacing aragonite is typically coarse, irregularly shaped crystals that cut across original fabrics and often contain aragonite inclusions. This fabric is not found in shrubs examined in the Kwanza Basin, although there are some shrubs with prismatic calcites that appear replacive (Figure 7D). Although shrubby calcites contain high strontium concentrations similar to elevated strontium concentrations in

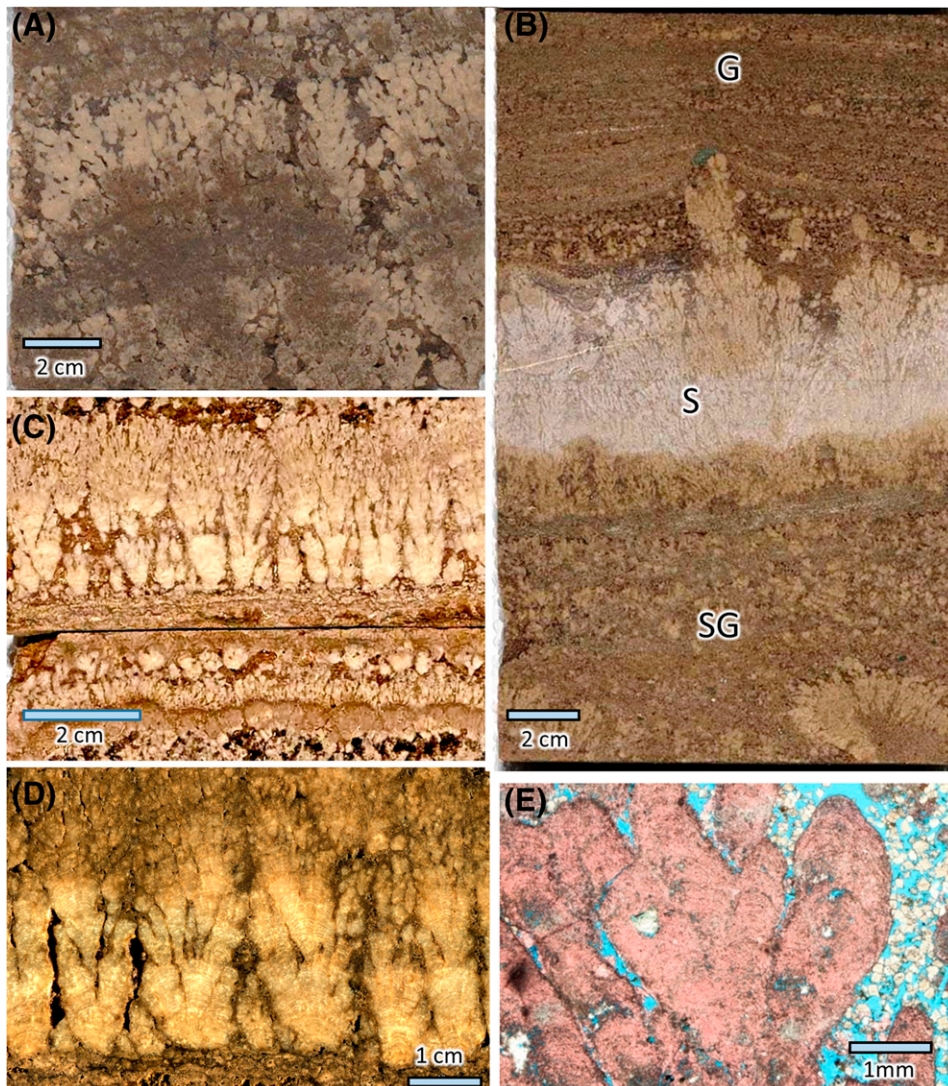


Figure 6. Core photographs (A–D) and photomicrograph (E). (A) Dendritic shrubby growth. (B) Dendritic shrubby growth (S) is overlain by intraclastic grainstone (G) with one shrub growth that grew above the others. Shrubs grew on a grain-rich layer with incipient shrubby growths (SG). (C) Intervals of dendritic shrubs alternating with grain-rich layers. (D) Close up of dendritic shrub showing vuggy porosity between shrubs. (E) Shrubby calcitic growth (red) with dolomite crystals (white to light brown) in pores between shrub growths. Stained with Alizarin Red S causing calcite to appear red. Porosity is blue.

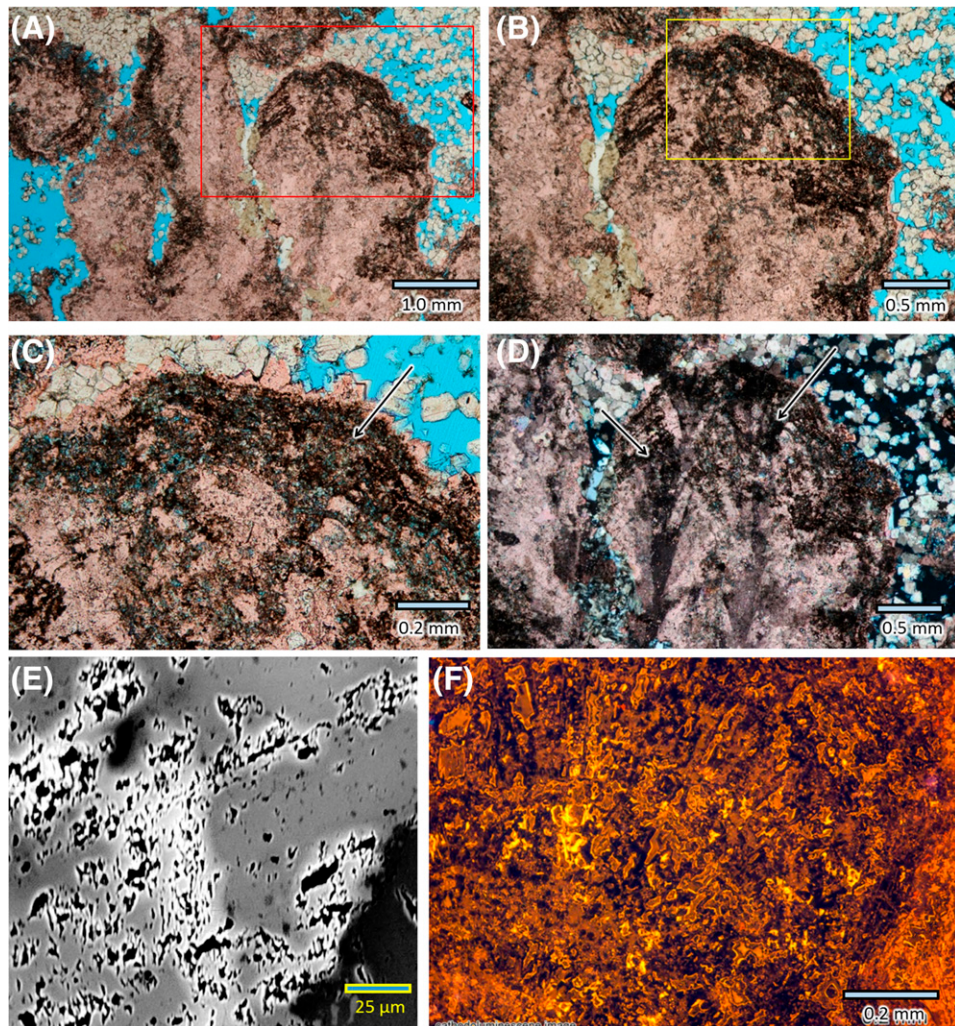
neomorphosed marine aragonite (Saller, 1992), the presalt lake waters probably contained high amounts of dissolved strontium, making it possible to incorporate the high amount of strontium observed in the shrubs by calcite precipitated directly from lake water. Even the best-preserved shrubs have a spotted cathodoluminescent pattern (Figure 7F) indicating that they had some transformation. The shrubs likely were originally deposited as magnesium (Mg)-rich calcites and have transformed to low-Mg calcite.

Microbial Chert Boundstone and Lithoclast Breccia (Talus)

Microbial chert boundstones and chert lithoclast breccias are commonly interbedded and hence are

described and interpreted together. Microbial chert boundstones frequently form isolated buildups basinward of sag platforms and occur as buildups on the basinward margin of platforms (Figure 4). On slabs, this facies ranges from light brown to dark gray and forms pillars, thick branches (2–10 cm [0.8–3.9 in.] across), domes, and layers (Figure 8). Primary vuggy porosity is common in the chert microbialites. The chert is frequently fractured, unlike adjacent dolomites and limestones. Chert-rich microbial boundstones commonly alternate with dolomite. The chert often shows a clotted texture (microporous or dark brown; Figure 9A–C) that is reminiscent of microbial structures described by Chafetz and Guidry (1999), Guidry and Chafetz (2003), and Scholle and Ulmer-Scholle (2003). The chert has an open, porous fabric showing no signs of compaction. The dark-brown

Figure 7. (A–D) Photomicrographs of shrubby calcitic growths (pink) with dark microcrystalline bands and dolomite (white-to-light-brown crystals) between shrubby growths. Stained with Alizarin Red S causing calcite to appear red. Pore spaces are blue. (A) Area in red rectangle is shown in (B). (B) Area in red rectangle in (A). Area in yellow rectangle is shown in (C). (C) Close up of yellow rectangle in (B). Note dark microcrystalline alteration bands at end of shrubby growth (arrow). (D) Cross-polarized view of (B). Prismatic crystals (arrows) indicate recrystallization. (E) Back-scatter image showing inclusions in a shrub that are oriented parallel to crystal growth (to upper right). (F) Cathodoluminescence image showing patchy luminescence in a shrubby growth with fibrous crystals.



clots are surrounded by transparent, microcrystalline quartz (Figure 9A), and the larger pores are lined with layers of botryoidal, colloform chalcedony (Figure 9C). Some cherts contain abundant spherical bodies, 20 μm across (Figure 8D), that are similar to silicified cyanobacteria (coccoid *Pleurocapsa*) found in chert in modern Lake Magadi, Kenya and shown in Behr (2002). The fractures in the chert appear randomly oriented, and many are open, whereas others are partially filled with sediment and calcite cement (Figure 9D). Results of $\delta^{18}\text{O}$ analyses on cherts are shown in Figure 9E and Tables 2 and 3.

Lithoclast breccias are frequently associated with cherty microbial boundstones. Most clasts are angular microbial cherts, some with truncated chalcedony cements (Figure 9F). Clasts range in size from less than 1 mm (0.04 in.) to tens of centimeters across. Crusts of chalcedony cements grew on clasts, significantly reducing interclast porosity (Figure 9F); however,

significant porosity remains between clasts. Some clasts have layers of chalcedony that were truncated by erosion prior to deposition in the breccia (Figure 9F).

At this time, we do not have good modern or ancient analogs for these microbial chert buildups. Morphologically, these pillars and branching forms with microbial structures are similar to Pavilion Lake (British Columbia, Canada) buildups (Laval et al., 2000), but those are calcitic. These microbial chert mounds amalgamate to form buildups that are seismically mappable, being as much as 200 m (656 ft) thick and 1–2 km (0.6–1.2 mi) across. Those microbial chert buildups coalesce into reefal structures that are more than 10 km (6 mi) long and more than 5 km (3 mi) wide. Silica (chert) precipitated in microbial mats was described by Al Rajaibi et al. (2015) in the Proterozoic of Oman, but those microbially mediated cherts formed in relatively thin layers, not thick, reef-like mounds.

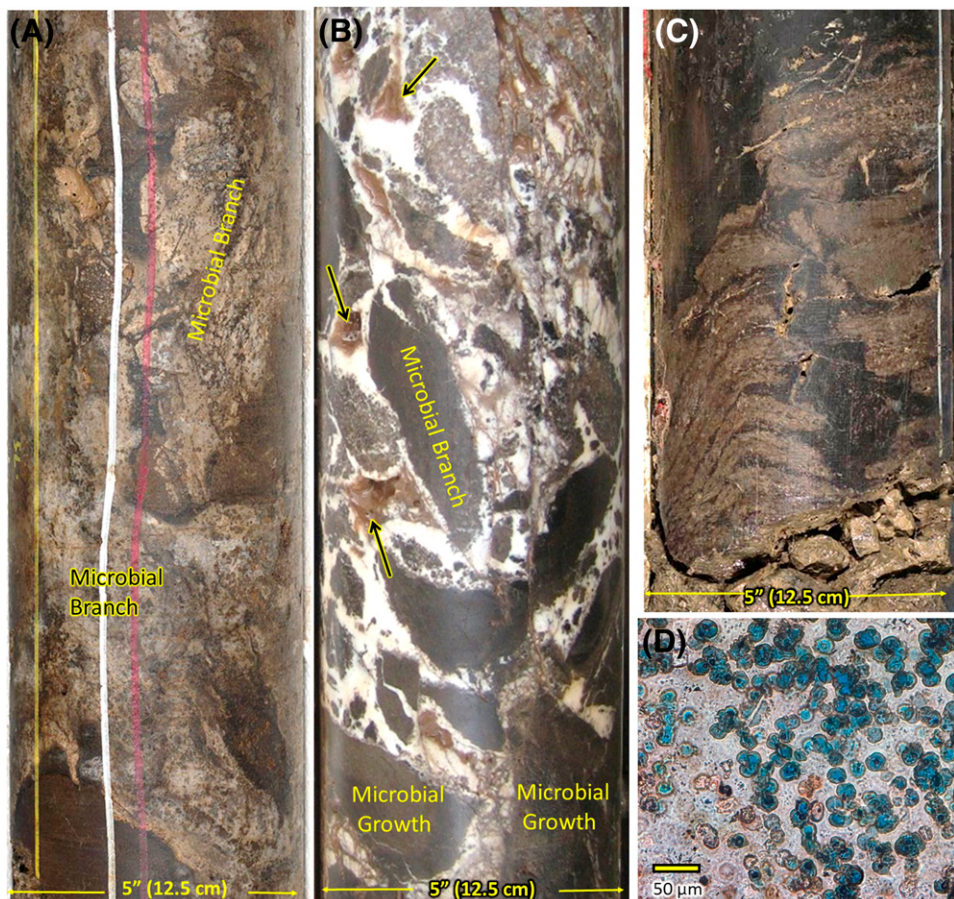


Figure 8. Core photographs of microbial chert facies. (A) Thick “branches” of microbial chert (light brown) in a dark-brown dolomite matrix. Branches have fractures filled with dark dolomite. (B) Boundstone with dark microbial branches and “vase-like” growths at the bottom. White crusts of chalcedony and quartz cement partially filled vugs between microbial chert. Some vugs remain open (arrows). This piece of core also has many open fractures. (C) Domal microbial chert (light to medium brown). (D) Thin-section photomicrograph of chert. Microcrystalline quartz is white. Small spherical bodies approximately 20 μm in diameter are filled with blue plastic. Many of the spherical bodies contained small air bubbles (now blue). These are similar to the microbial reproductive cells (baeocytes) of Behr (2002).

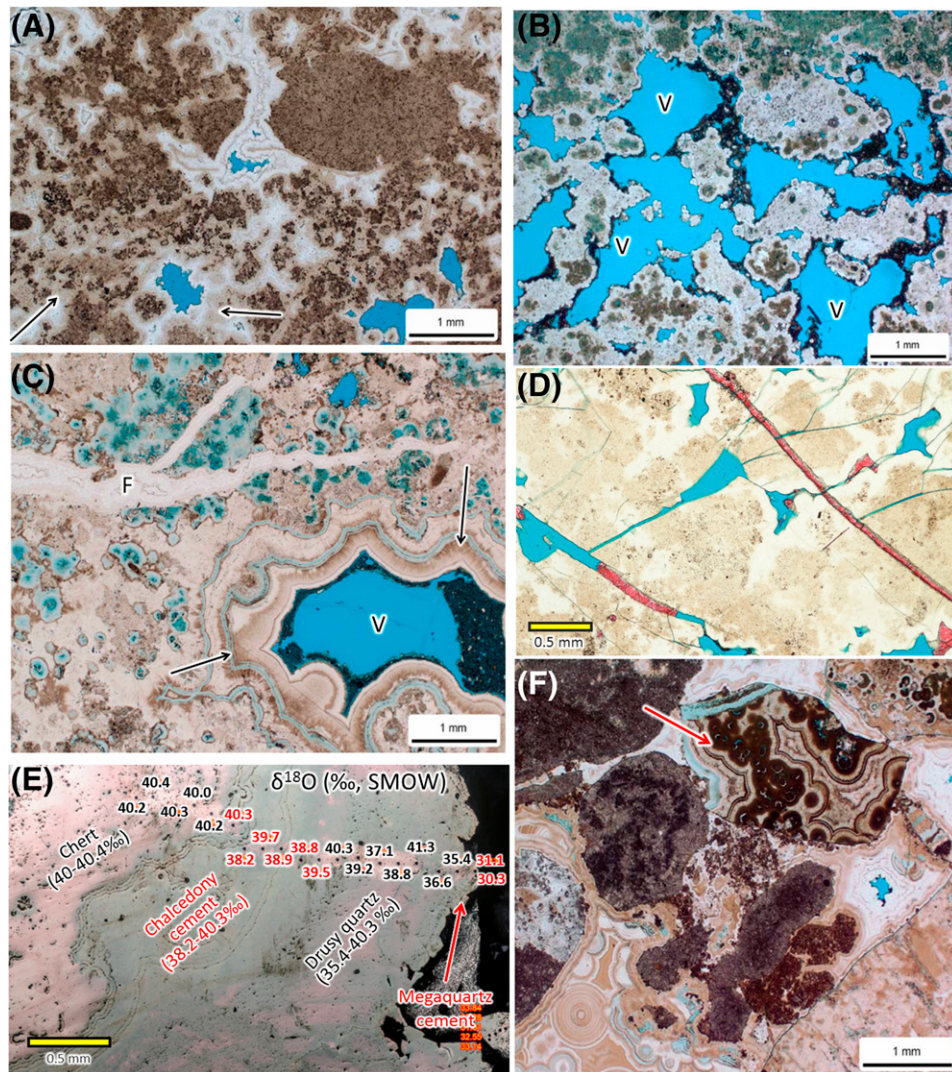
Petrographic and stable isotopic data indicate that these microbial chert boundstones grew as reefs at low (surface) temperatures. Petrographically, most vugs appear to be depositional, generally lacking truncations typical of dissolution. The breccias are interpreted as “reef talus” because of the poor sorting and angular nature of the clasts. The clasts are generally reefal material (microbial chert boundstones). Clasts contain truncated layers of chalcedony cement, indicating that the chalcedony cements grew syndepositionally and were eroded (Figure 9F). The general absence of ostracods and mollusks suggests very saline or alkaline lake waters.

Lake Magadi chert shows some petrographic similarities to these cherts, but they do not form isolated buildups or reefs along margins of platforms. The spherical reproductive cells or baeocytes are found in the Lake Magadi chert and modern lake water and exhibit an internal concentric structure (capsule), whereas most of those Kwanza structures are molds. The Magadi capsules are 5 to 20 μm in diameter (similar to ours); the larger capsules are inferred to grow under conditions of high evaporation, high salinities,

periodic desiccation, and intense ultraviolet radiation; the smaller capsules lived in deeper waters (Behr, 2002). These cherts are associated with cyanobacteria mats. Chalcedony is also common in the siliceous sediment and gels in Lake Magadi (Behr, 2002).

The clotted chert and early chalcedony cements commonly have $\delta^{18}\text{O}$ values of approximately +40‰ (standard mean ocean water [SMOW]; Figure 9E; Tables 2 and 3). Cherts from the saline lakes of East Africa show similar high isotope ratios. Higher $\delta^{18}\text{O}$ values are correlated with rising salinity. Exceptionally high $\delta^{18}\text{O}$ values (39‰ to 44‰, SMOW) were obtained for Lake Magadi chert by O’Neil and Hay (1973), who also found saturated Lake Magadi water to have $\delta^{18}\text{O}$ values of 7‰ (SMOW), whereas warm spring waters were approximately -3‰ (SMOW). Assuming that the Kwanza surface waters had a temperature of 25°C (77°F), chert with a $\delta^{18}\text{O}$ value of 40‰ (SMOW) would precipitate from water with a $\delta^{18}\text{O}$ of approximately 6‰ (SMOW), indicating similar highly evaporated water (Figure 10; Ligang et al., 1989). This makes a hydrothermal origin for the

Figure 9. Thin-section photomicrographs of chert facies. (A) Chert with clotted dark-brown microbial structures, with crusts of chalcedony cement (light brown; arrows) and quartz cement (white). Residual vuggy porosity remains (blue). (B) Chert with clotted microbial structures (blue brown where microporous). Quartz cement (white) coats the microbial fabric. Vuggy porosity remains (V; blue). (C) Microbial boundstone. Chert with clotted microbial structures (brown or blue brown where microporous). Chalcedony cements (arrows; light brown to light blue where microporous) partially fill a vug (V). An irregular fracture (F) is filled with quartz cement. (D) Fractured chert. Fractures are partially filled by calcite cement (red) and partially open (blue). Fractures have multiple orientations. Stained with Alizarin Red S. (E) Reflected-light photograph of chert, chalcedony cement, and quartz cement showing oxygen isotope ($\delta^{18}\text{O}$) results from ion probe isotopic analyses. (F) Intraclast-lithoclast breccia with layers of chalcedony (light brown) and quartz cement (white). Clast (arrow) with truncated chalcedony cements indicates syndepositional precipitation of silica cements. SMOW = standard mean ocean water.



Kwanza cherts highly unlikely, because an increase in temperature would require an even higher $\delta^{18}\text{O}$ value for the water; cherts in hydrothermal sinters from Yellowstone have $\delta^{18}\text{O}$ values of 6‰ to 22‰ (SMOW; Shanks et al., 2007).

The open vugs in the Kwanza chert are often lined by megaquartz crystals. The youngest (last) parts of these crystals have $\delta^{18}\text{O}$ values approaching 30‰ (SMOW; Figure 9E; Table 3). The present subsurface formation waters have $\delta^{18}\text{O}$ values of approximately 4‰ (SMOW), so quartz would precipitate at a temperature of approximately 66°C (150°F) from those waters (Figure 10). The present formation temperature is approximately 95°C (203°F), implying that quartz precipitation stopped before the formation

reached its present burial depth. Uncertainties exist for these quartz calculations: (1) precipitation is required to be at equilibrium (reasonable for these euhedral crystals), and (2) several quartz–water fractionation equations are available; hence, the Ligang et al. (1989) equation that we used might not be exactly appropriate.

Layered Spherulite–Intraclast Packstone–Grainstone

Spherulite–intraclast packstone–grainstones occur on sag platforms in the Kwanza Basin (Figures 4, 11) and are generally calcitic, but sometimes they contain dolomite. Some of the packstone–grainstones are

Table 2. Oxygen Isotope Laser Fluorination Analyses of Bulk Rock Silica Samples

Number	Type of Silica	$\delta^{18}\text{O}$ (SMOW)
1	Chert	36.9‰
2	Chert	41.4‰
3	Chert	38.9‰
4	Light brown chert	41.2‰
5	Dark brown chert	44.6‰

Abbreviations: SMOW = standard mean ocean water.

dominated by intraclasts, but others are dominated by spherulites, and still others are a mixture of intraclasts and spherulites. (Spherulites are small, spherical grains composed of radiating fibrous-to-prismatic calcite crystals; Wright and Barnett, 2015.) Intraclasts include fragments of shrubs and hybrid carbonate grains that are intermediate between spherulites and shrubs.

Some of the spherulites and hybrid grains were probably moved by currents, whereas others appear to have grown and been deposited “in place.” Intergranular porosity is common in this facies (Figure 11).

Our interpretation is that lack of mud (carbonate or siliceous) suggests deposition in an environment where currents prevented deposition of mud. Presence of intraclasts indicates that currents capable of eroding and transporting grains more than 0.2 mm (0.008 in.) across were active. Hence, the spherulite–intraclast packstone–grainstones are interpreted as being deposited in a shallow environment with frequent, strong currents.

Spherulite Wackestone–Packstone

Spherulite wackestone–packstones (Figures 4, 12) are a common facies in the sag interval. Spherulites range

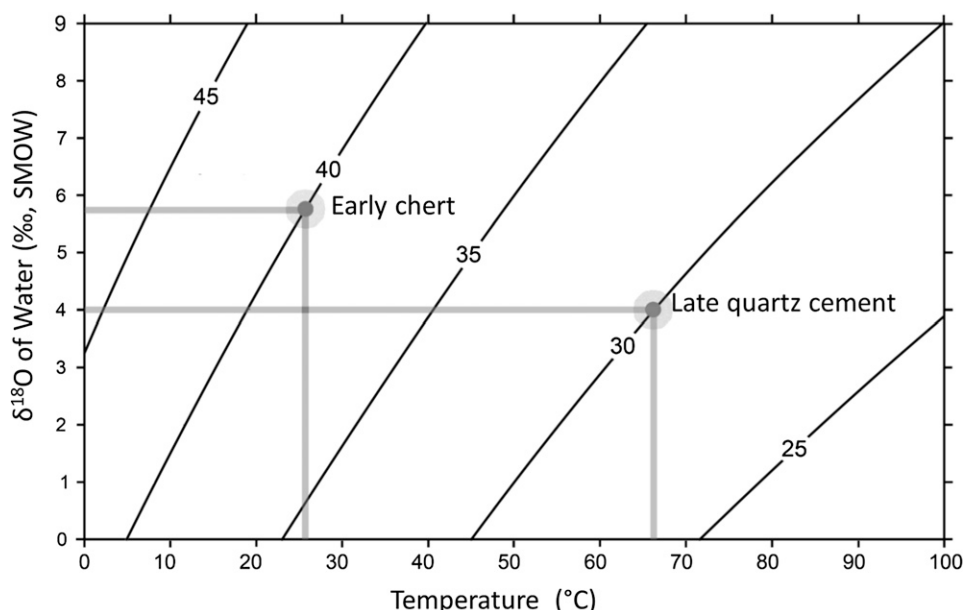
Table 3. Oxygen Isotope (Secondary Ion Mass Spectrometry) Analyses for Sequence of Silica Minerals Shown in Figure 9E

Point	Type of Silica	$\delta^{18}\text{O}$ (SMOW)	Standard Error (‰)
1	Chert	40.2‰	0.248
2	Chert	40.4‰	0.287
3	Chert	40.3‰	0.279
4	Chert	40.0‰	0.400
5	Chert	40.2‰	0.353
6	Cement band of chalcedony	40.3‰	0.312
7	Cement band of chalcedony	38.2‰	0.446
8	Cement band of chalcedony	39.7‰	0.265
9	Cement band of chalcedony	38.9‰	0.422
10	Cement band of chalcedony	38.8‰	0.461
11	Cement band of chalcedony	39.5‰	0.340
12	Drusy quartz	40.3‰	0.348
13	Drusy quartz	39.2‰	0.343
14	Drusy quartz	37.1‰	0.383
15	Drusy quartz	38.8‰	0.367
16	Drusy quartz	41.3‰	0.323
17	Drusy quartz	36.6‰	0.362
18	Drusy quartz	35.4‰	0.282
19	Megaquartz	31.1‰	0.191
20	Megaquartz	30.3‰	0.118
21	Megaquartz	33.8‰	0.361
22	Megaquartz	33.3‰	0.345
23	Megaquartz	31.8‰	0.315
24	Megaquartz	32.6‰	0.349
25	Megaquartz	33.1‰	0.373

The first sample point is in replacement chert (on the left); the last sample point is in megaquartz against open pore (on the right).

Abbreviations: SMOW = standard mean ocean water; $\delta^{18}\text{O}$ = oxygen isotope.

Figure 10. Graphical representation of equilibrium relationship between oxygen isotope ($\delta^{18}\text{O}$) value of water, temperature, and the $\delta^{18}\text{O}$ value of quartz from Ligang et al. (1989). The curves indicate the isotope ratio of the solid (quartz) in per mil relative to standard mean ocean water. The secondary ion mass spectrometry probe analysis points for $\delta^{18}\text{O}$ are shown in Figure 9E and given in Table 3. Possible equilibrium points for a chert with a $\delta^{18}\text{O}$ value of 40‰ and a quartz with a $\delta^{18}\text{O}$ value of 30‰ are shown. SMOW = standard mean ocean water.



in size from silt to sand (0.03–2 mm [0.001–0.08 in.] across). The material between the spherulites ranges from clay-rich mud (stevensite) to coalescing dolomite crystals. Spacing between spherulites ranges from coalesced spherulites to widely spaced spherulites surrounded by dolomite or clay (Figures 3D, E; 12E, F). Spherulites are locally dolomitized, though they are most commonly calcite.

Spherulites have been interpreted to form in muddy sediments or gels at the sediment–water interface involving waters supersaturated with respect to calcite (Tosca and Wright, 2015; Wright and Barnett, 2015). Both muddy sediments and gels require lake waters deep enough to have little current agitation. The absence of ostracods and mollusks suggests a very stressed environment (probably saline and alkaline lake waters).

Stevensite (Clay) with Calcitic Spherulites or Dolomite Rhombs

Stevensite with calcitic spherulites or dolomite rhombs is a common facies in the sag interval (Figure 3D–G). Stevensite is an aluminum-poor, Ca–Mg smectitic clay. Spherulites or dolomite rhombs range in abundance from very sparse to touching and grade to spherulitic wackestone–packstones and crystalline dolomites. This facies is commonly laminated, with clays compacting around the spherulites or dolomite rhombs. Stevensite is generally more abundant in areas off structural highs.

Stevensite precipitates in highly alkaline lake waters ($\text{pH} > 9$; Khoury et al., 1982; Jones, 1986; Tosca and Wright, 2015). Precipitation of calcitic spherulites indicates that these waters were also calcium rich and supersaturated with respect to calcite, and precipitation with dolomite indicates lake waters that were magnesium rich and hence supersaturated with respect to dolomite. The abundance of clay in this facies supports deposition in a low-energy environment with no significant currents to winnow the clay out. The abundance of stevensite off structure suggests deposition mainly in deeper water. Hence, the stevensite facies was generally deposited in deeper parts of silica-rich, highly alkaline lakes.

Crystalline Dolomite

Crystalline dolomite beds are commonly associated with and gradational to spherulite wackestones, stevensite mudstones, or organic mudstones. The crystalline dolomites generally lack grains and may contain clay (Figure 3A). The dolomite crystals are generally euhedral and widely spaced in these crystalline dolomites. (Crystalline dolomites lack features indicative of replacement, i.e., replaced grains.)

Our interpretation is that the presence of widely spaced crystals suggests precipitation of dolomite directly from lake water supersaturated with respect to dolomite. No evidence of currents exists. Evidence for the lack of currents includes interbedding with

deeper-water facies (stevensite-rich or organic-rich mudstones) and the presence of mud, which suggests deposition in waters that lacked strong currents.

Intermediate “Hybrid” Facies

The sag interval contains some transitional grain types and facies that do not fit into the categories above. Strata with irregular calcitic grains that appear to be hybrids of spherulites and shrubs (Figure 13A, B) are widespread and occur in wackestones, packstones, grainstones, and shrubby boundstones. Coalescing, fibrous calcite crystals that are similar to “botryoidal” marine cements (Figure 13C) occur in some samples.

Our interpretation is that the sag lake was, at least at times, supersaturated with respect to calcite. The exact morphology of calcitic precipitate was a function of depositional water energy, degree of supersaturation, and substrate, with spherulites growing in muddy sediments and shrubs growing in shallow, high-energy, highly supersaturated environments. The hybrids of spherulites and shrubs probably formed in transitional (in time or space) environments between low-energy muddy and high-energy grain-rich or shrub-rich sediments. The botryoidal cements, which are fairly rare, could have precipitated in an internal reefal cavity or perhaps at the sediment–water interface, similar to shrubs.

UPPER SYNRIFT FACIES

Because our drilling has focused on structural highs in the presalt, most wells have not penetrated the lower synrift interval that is generally confined to grabens in the Kwanza Basin (Figure 4). Shallow water strata in the upper synrift interval are very different from the sag. Upper synrift facies were deposited in the late stages of rift-related faulting and are generally upper Barremian (ostracod stages AS9–AS10). Most upper synrift strata on depositional highs are limestones with mollusks, especially bivalves (Figure 4).

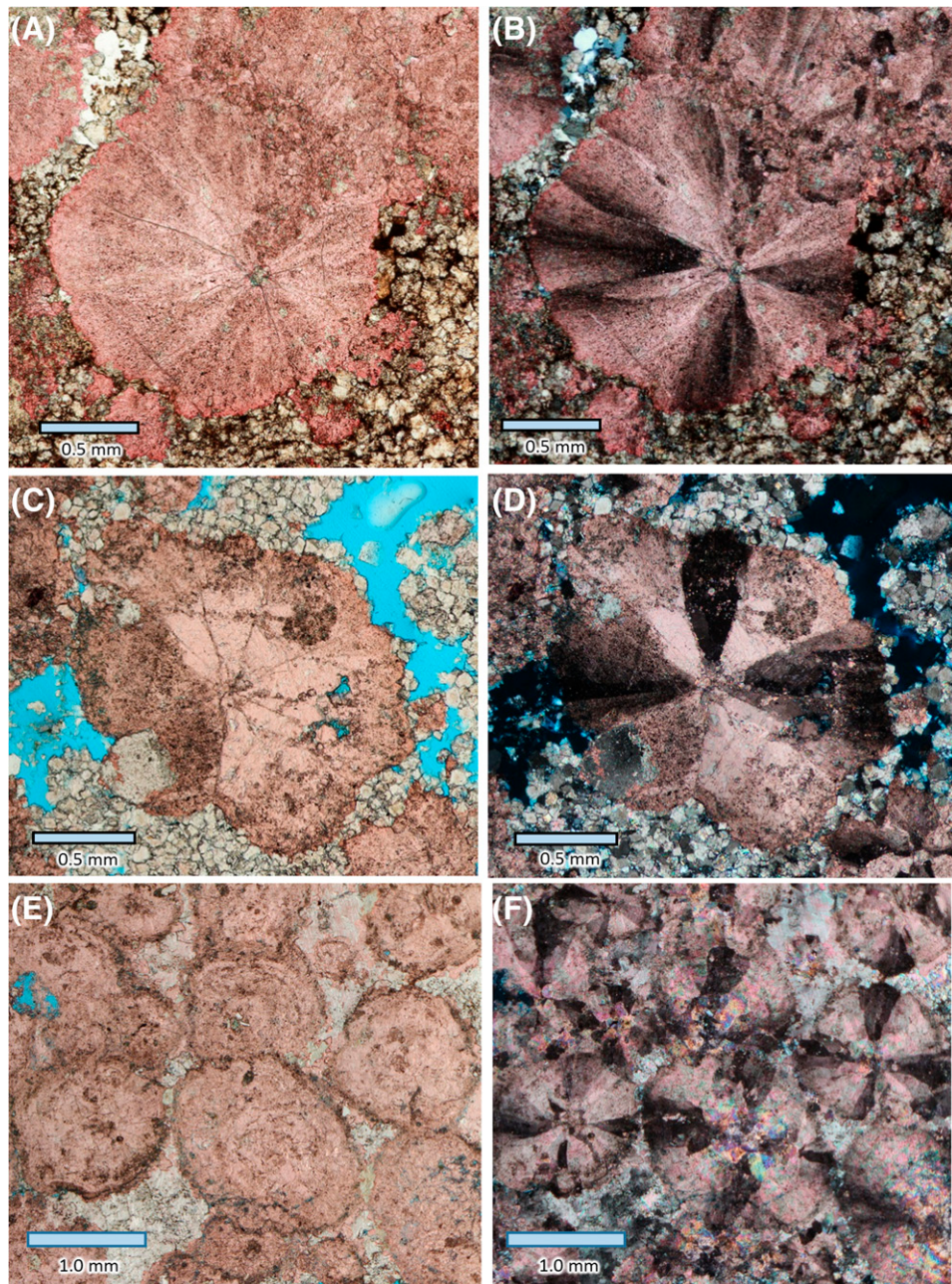
Mollusk Grainstones, Packstones, and Wackestones

Upper synrift strata on structural highs in the Kwanza Basin contain mollusk grainstones, packstones, and



Figure 11. (A) Core photograph of a current laminated intraclast-spherulite grainstone. (B) Thin-section photomicrograph of a porous intraclast grainstone. Stained with Alizarin Red S causing calcite to appear red. Porosity is blue.

Figure 12. Thin-section photomicrographs of spherulites in the sag interval. Stained with Alizarin Red S. Calcite appears red, and porosity is blue. (A) Calcitic spherulite with radiating bundles of fibrous crystals in an argillaceous dolomite matrix. (B) View of (A) under cross-polarized light showing radiating bundles of fibrous crystals. (C) Calcitic spherulite with wedge-shaped calcite crystals. Dolomite (light brown) and porosity (blue) are adjacent to spherulites. (D) View of (C) under cross-polarized light showing wedge-shaped crystals in the spherulite. (E) Calcitic spherulites (red) with radiating bundles of fibrous crystals and wedge-shaped crystals. Space between spherulites is filled with dolomite (light brown). (F) View of (E) under cross-polarized light showing radiating bundles of fibrous crystals and wedge-shaped crystals.



wackestones (Figures 14A, B; 15A–F). Mollusk grainstones and packstones are commonly referred to as “coquinas.” Mollusks include bivalve and gastropod shells. Bivalves occur as whole shells and fragments, and they are the dominant grain type in most synrift grainstones, packstones, and wackestones. Gastropod shells are abundant in a few intervals. This facies is dominantly limestone with some dolomite (Figures 14B, 15G) and silicified intervals. A few ostracods are present in this facies (Figure 15F), but, except for a few intervals, they are not volumetrically significant.

Thompson et al. (2015) provides an excellent summary of coquinas in the Lower Cretaceous of the South Atlantic and modern environments. The presence of mollusks indicates a lake with moderate-to-low salinities (for example, mollusks are not present in highly saline lakes like the Great Salt Lake, Utah; Eardley, 1938). Grainstones were probably deposited in high-energy environments or at least during high-energy events. Mollusk packstones with whole shells could have accumulated in an area with abundant living mollusks. The mollusk packstones may have also been

deposited by episodic currents. Mollusk wackestones were deposited in relatively quiet waters (low energy).

Other Upper Synrift Facies

Although mollusk-rich strata are the main facies in the upper synrift, some other facies are present. Ostracods (Figure 15F) are concentrated in wackestones, packstones, or grainstones in a few beds, though these beds are relatively rare in the upper synrift. Unfossiliferous dolomites occur in the uppermost part of this interval. Dolomitic mudstones and silicified ooid packstones and grainstones are also present in a few other intervals in the upper synrift.

Ostracods can live in environments deeper and more saline than mollusks, and they can become abundant in those stressed environments (Flügel, 1982; Scholle and Ulmer-Scholle, 2003). Hence, ostracods in the absence of mollusks suggest an environment either relatively deep or very saline. Ostracods are small, so even gentle currents can move them and winnow out muds, forming ostracod grainstones. Ostracod wackestones and packstones could have accumulated in deeper, low-energy environments. The absence of mollusks and ostracods in dolomitic mudstones suggests times when the upper synrift lakes became too saline for mollusks and ostracods. Ooid grainstones probably accumulated in lacustrine environments with continual or repeated agitation, similar to some windward coastlines in the modern Great Salt Lake (Eardley, 1938).

FACIES PRESENT IN BOTH SAG AND UPPER SYNRIFT

Several siliciclastic facies are present in both the synrift and sag intervals. Sandstones, siltstones, conglomerates, and those same lithologies mixed with shells are found in the synrift and sag intervals in

Figure 13. Thin-section photomicrographs. Thin sections were stained with Alizarin Red S causing calcite to be red. (A) Irregular “hybrid” calcitic grain (pink) showing preferential upward growth causing a grain that is intermediate between a shrub and a spherulite. Dolomite (light brown) fills spaces between calcitic grains. (B) View of (A) under cross-polarized light showing radiating bundles of fibrous crystals. (C) Coalescing botryoids of fibrous cements. All dolomite. Cross-polarized light.

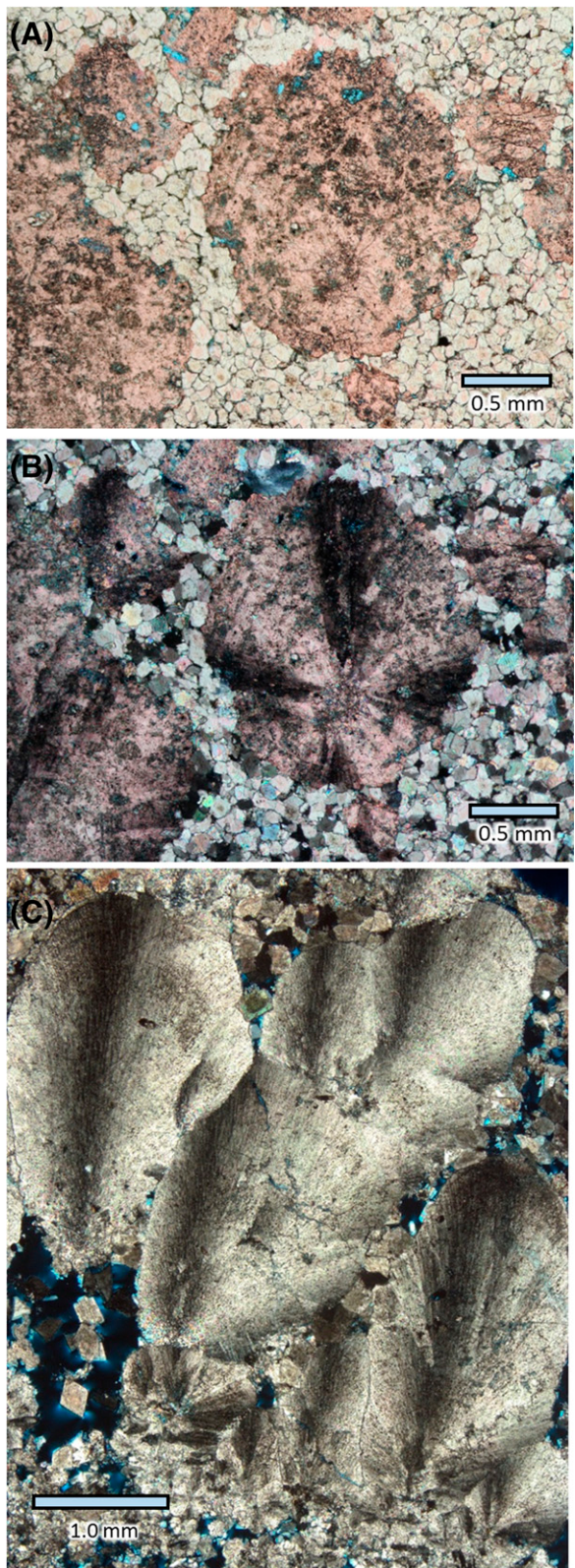
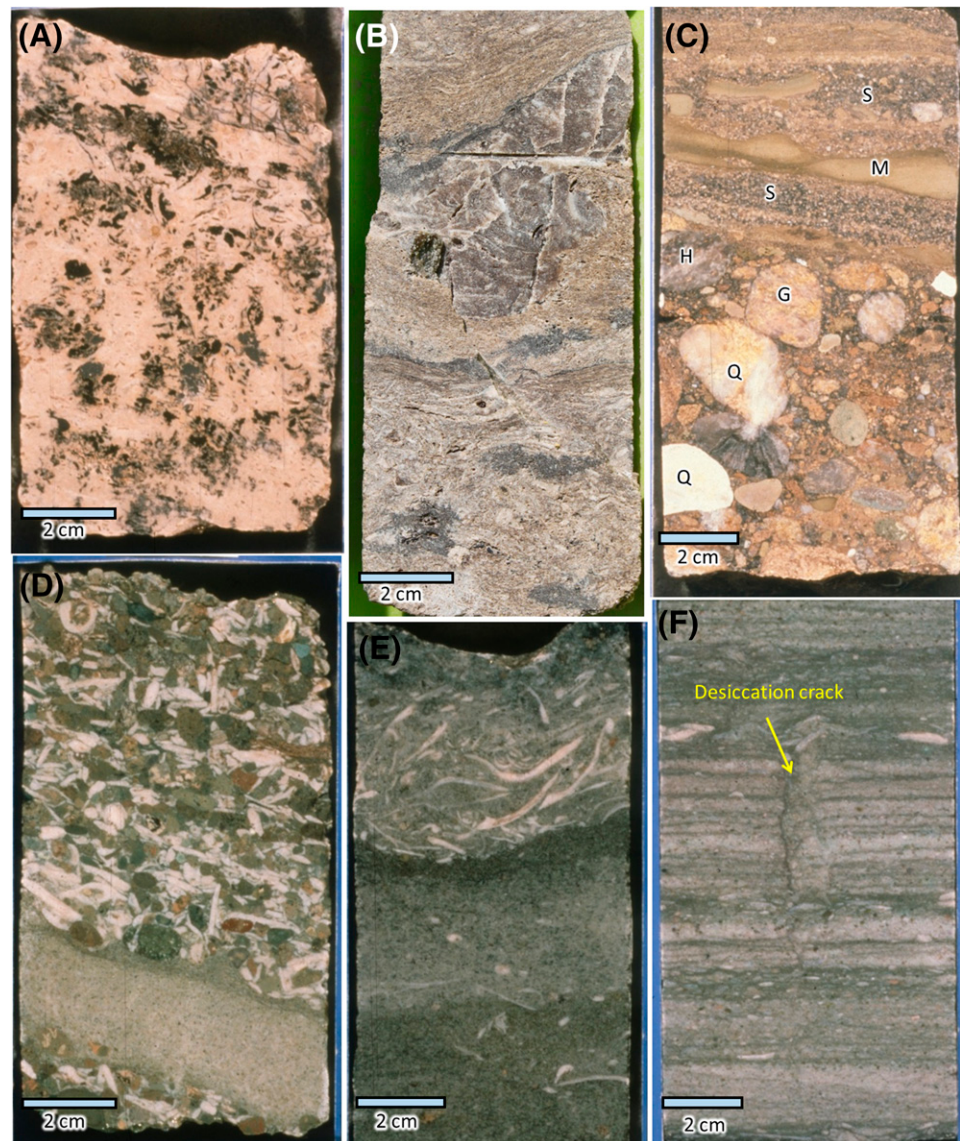


Figure 14. Core photographs of presalt facies. (A) Mollusk packstone with leached shells causing moldic porosity. Black color is caused by oil staining. (B) Dolomitized mollusk packstone-grainstone with open vugs and fractures. (C) Conglomerate with sandstone (S) and siliciclastic mudstone (M). Clasts include quartzite (Q), gneiss (G), and schist (H). (D) Conglomerate with green sandstone and siltstone clasts and thick white mollusk shells. (E) Green fine-grained sandstone with whole bivalve shells. (F) Laminated silt-rich and lime-rich mudstone with a syn-depositional desiccation crack filled with sediment.



eastern parts of the basin. Organic-rich mudstones and clay-rich mudstones also occur in both the upper synrift and sag in many parts of the Kwanza Basin.

Conglomerate and Coarse Sandstone

Conglomerates and coarse sandstones (Figure 14C) are observed in more landward areas of the Kwanza Basin in both synrift and sag intervals (Figure 4). Clasts in conglomerates are up to 10 cm (4 in.) across and include metamorphic gneiss as well as siliceous mudstone and limestone clasts. Conglomerates are commonly massive or show upward fining to sands (Figure 14C). Sandstones are coarse to fine grained, and many have current laminations.

Most conglomerates and sandstones are interpreted as deposited in fluvial-to-alluvial fan environments. This interpretation is suggested by their (1) coarse grained nature, (2) local upward fining, (3) local current laminations, (4) deposition in landward parts of the basin, and (5) lack of calcareous fossils indicative of lacustrine environments.

Shelly Conglomerate and Sandstone

The shelly conglomerate and sandstone facies was also observed in more landward parts of the Kwanza Basin (Figure 14D). Clasts in conglomerates are up to 5 cm (2 in.) across and include clasts of metamorphic gneiss. Thick calcareous mollusk shells are also present.

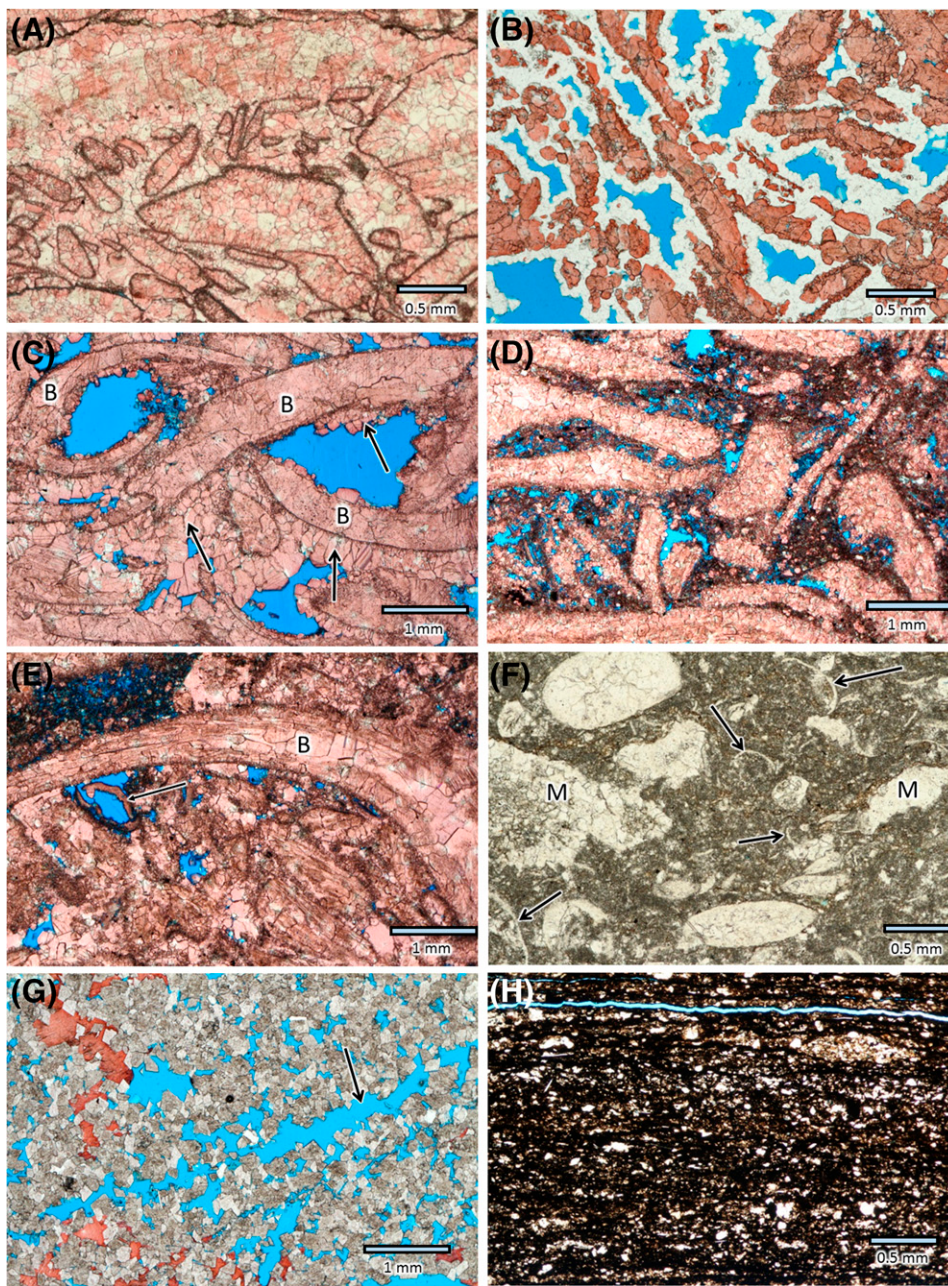


Figure 15. Thin-section photomicrographs of synrift strata. All views except (F) were stained with Alizarin Red S, and calcite is red. (A) Grainstone composed of mollusk fragments with equant calcite cements filling primary intergranular porosity. Mollusk fragments were dissolved and then filled with equant calcite cement. (B) Mollusk grainstone with neomorphosed shell fragments. Intergranular pores are lined with quartz cements (white), and substantial intergranular porosity remains (blue). (C) Mollusk grainstone with neomorphosed bivalve shells (B) and intergranular porosity (blue). Intergranular porosity was reduced by calcite cement (arrows). (D) Mollusk packstone with bivalve shells and fragments, intergranular micrite (dark), and porosity (blue). (E) Mollusk packstone–grainstone with neomorphosed bivalve shells (B), an ostracod (arrow), and open pores (blue). (F) Lime wackestone with mollusk fragments (M) and ostracod shells (arrows) in lime mud (dark). (G) Porous dolomite with a dissolved mollusk shell (elongate pore; arrow) and late calcite cement (red). (H) Laminated silty, dolomitic, organic-rich mudstone.

Sandstones are coarse to fine grained, and many have current laminations.

Thick mollusk shells are indicative of shallow, fresh-to-relatively low-salinity lacustrine environments similar to Lake Tanganyika, East Africa (Cohen and Thouin, 1987; Cohen, 1989). The coarse siliciclastic material is typical of fluvial deposits. The mixture of mollusk shells and coarse siliciclastic grains suggests episodic input of coarse siliciclastic sediment into a lake. This mixture of sediment is common in “fan deltas,” where alluvial sediments are carried into the margin of a lake or ocean.

Green Fine Sandstone and Siltstone

The green fine sandstone and siltstone facies (Figure 14E) is present in wells in the landward parts of the basin in both synrift and sag intervals. These strata are horizontally laminated in some intervals and bioturbated in other intervals. Mollusk shells are present in some parts of this facies.

The presence of mollusk shells suggests deposition in the shallow part of a lake. Abundant sand and silt indicate proximity to an active siliciclastic source. This facies is interpreted as being

deposited on the landward side of a lake margin in the eastern part of the basin.

Light-Colored Mudstone

Light-colored mudstones are present in some land-ward (eastward) wells (Figure 14F). Millimeter laminations, thicker (centimeter) layering, and synsedimentary disruption (cracks) are present. This facies is generally unfossiliferous.

Our interpretation is that the abundance of mud suggests a low-energy environment. Fine laminations suggest episodic deposition. The light gray and brown color suggests an oxidized depositional environment. Cracks filled with sediment (Figure 14F) are consistent with brief exposure and desiccation. This facies was probably deposited on mud flats at or slightly above the average lake level.

Organic-Rich Mudstone

Organic-rich mudstones (Figure 15H) are a critical part of the Kwanza Basin petroleum system. These mudstones are dark and have total organic carbon contents of 1–10 wt. %. Organic material is commonly amorphous kerogen with high hydrogen indexes typical of lacustrine deposition and similar to the Bucomazi Formation (Hauterivian–Aptian; Figure 2) in the Lower Congo Basin (Schoellkopf and Patterson, 2000). The mudstones range from dolomitic to calcareous to clay rich. The mudstones are commonly unfossiliferous; however, some contain significant amounts of calcitic ostracods. Organic-rich mudstones occur in both the synrift and sag intervals (Barremian to lower upper Aptian).

Organic-rich mudstones are observed accumulating in deeper water in modern East African Rift lakes (Scholz et al., 2003). Similar organic-rich mudstone facies in the Bucomazi Formation of northern Angola are interpreted as deposited in deeper, anoxic lacustrine environments (Harris, 2000; Schoellkopf and Patterson, 2000). Hence, organic-rich mudstone facies in the presalt of the Kwanza Basin are interpreted as deposited in deep lacustrine environments. These are the main source rocks in the presalt.

Siliceous Mudstone

Siliceous mudstones range from pure clay to silt and sand rich to carbonate rich. They occur as interbeds in the synrift and in deeper-water areas of the sag. Sometimes the siliceous mudstone facies contains spherulites or dolomite and has a gradational transition to dolomites and spherulitic wackestones.

Our interpretation is that siliceous mudstones accumulated in various presalt environments. Some siliceous mudstones are “autochthonous,” with clays precipitating directly from lake water, and hence are gradational to stevensite-rich facies described earlier. Other clays are detrital, the product of weathering, erosion, transportation, and deposition. The deposition of clay requires a “low-energy environment” with currents too weak to transport the clays. The preferential occurrence of stevensite on the flanks of structures suggests that those low-energy environments were deeper water, below wave base. Detrital clay could also be transported and deposited in deep water. Detrital clay could be associated with rivers and deposited on flood plains or delta fronts; however, we have not identified any clays deposited on flood plains or delta fronts, though we have little data in areas where we would expect this.

DIAGENESIS

Sag Diagenesis

Often, there is not a clear separation between precipitation of “depositional carbonate” and early diagenesis on the lake floor during sag deposition. For example, spherulites are interpreted to precipitate on the lake floor and in sediments during very shallow burial. In general, we will consider spherulites and shrubby microbial material as depositional and adjacent dolomite as slightly later and diagenetic. Crystalline dolomites precipitated directly out of lake water are considered depositional. Thin sections, x-ray diffraction analysis, and well log analysis indicate that most of the middle and upper sag is a mixture of calcite and dolomite with an average of approximately 65% calcite and 30% dolomite, with the remaining 5% including clay, chert, sand, silt, and other materials. Some samples are composed entirely of calcite and others of dolomite, but most parts of the sag are mixtures.

Calcitic grains and microbial calcites generally precipitated early and form the framework of the rock. Dolomite occurs as crystals in pores, and in some areas it replaces original calcareous sediments and results in substantial porosity. In other areas, dolomite occludes porosity between calcitic grains. Early dolomite in the sag interval has relatively high $\delta^{18}\text{O}$ values of 1‰ to 5‰ (Peedee belemnite [PDB]) and $\delta^{13}\text{C}$ values of 1‰ to 3‰ (PDB) (Figure 16).

Dolomite is the main diagenetic product observed in the sag interval. Many other diagenetic products are present, but they are volumetrically minor and not discussed here. Much dolomite in the sag appears to form diagenetically early. Dolomite crystals adjacent to shrubs and spherulites contain manganese (up to 8000 ppm) and were probably precipitated during very shallow burial, when the pore water became separated from oxidized lake water. It is possible that a reducing environment and microbial mediation helped promote dolomite precipitation in the very shallow subsurface (Vasconcelos et al., 1995; Vasconcelos and McKenzie, 1997).

The sag dolomites have an average $\delta^{13}\text{C}$ value of 2.1‰ (10 samples; standard deviation = 0.4), which is similar to the spherulites and shrubs (Figure 16) and reflects the dissolved carbon in the lake water. The sag dolomites have an average $\delta^{18}\text{O}$ value of 2.2‰ (10 samples; standard deviation = 1.3). Uncertainty exists over the isotopic fractionation for oxygen in dolomite, but the high $\delta^{18}\text{O}$ values in the dolomite (maximum value of 4.4‰) support precipitation from evaporated lake water at 25°C–30°C (77°F–86°F; using equations in Friedman and O’Neil, 1977; Land, 1985), similar to the chert. Diagenesis in many parts of the sag interval is minor, perhaps because the connate waters during early and moderate burial were relatively saline and less reactive than freshwater.

Synrift Diagenesis

Diagenesis in much of the synrift is intense and includes calcite cementation, calcite and aragonite dissolution, calcitization (neomorphism) of originally aragonitic mollusks, dolomitization replacing calcitic material, saddle dolomite cements, replacive chert, silica cement, and stylolites. Equant calcite cements fill many intergranular pores and molds of originally aragonite grains (Figure 15A–E). Most mollusk shells have been

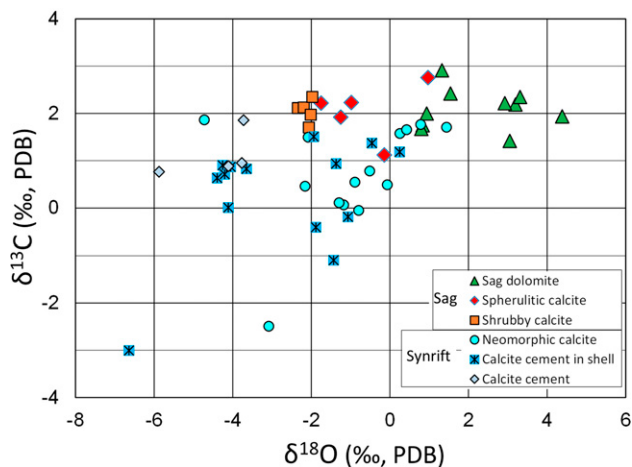


Figure 16. Stable isotope data from a well through a presalt carbonate platform. The synrift calcites have generally lower carbon isotope ($\delta^{13}\text{C}$) and oxygen isotope ($\delta^{18}\text{O}$) values than sag carbonates, though some overlap is present. PDB = Peedee belemnite.

either dissolved (Figure 14A), and sometimes infilled with equant calcite cement (Figure 15A, B, D), or calcitized (neomorphosed; Figure 15C, E). Dolomite has replaced some mollusk-rich limestones (Figures 14B, 15G). Saddle dolomite (coarse dolomite with curved cleavage planes and undulose extinction patterns) occurs in a few places as a paragenetically late, pore-filling cement. In the synrift, chert occurs as a replacive phase. Quartz cements are also present (Figure 15B). Stylolites, although relatively rare in the sag section, are more common in the synrift section.

The isotopic composition of diagenetic calcites is variable (Figure 16). Most neomorphic calcites have moderate $\delta^{18}\text{O}$ values (−2.5‰ to +2‰, PDB) and $\delta^{13}\text{C}$ values (−0.5‰ to +2‰, PDB). Calcite cements filling mollusk molds have $\delta^{18}\text{O}$ values of −5‰ to +0.5‰ (PDB) and $\delta^{13}\text{C}$ values of −1.5‰ to +1.5‰ (PDB). Calcite cements filling intergranular pores have lower $\delta^{18}\text{O}$ values (−6‰ to −3‰, PDB) and moderate $\delta^{13}\text{C}$ values (+0.5‰ to +2‰, PDB; Figure 16).

Our interpretation is that diagenesis of synrift strata occurred in the shallow subsurface as well as during deep burial. Freshwaters probably entered the synrift interval at the unconformity at the top of the synrift. It is likely that the synrift interval was also periodically exposed to freshwater during deposition. The $\delta^{18}\text{O}$ data separate the early freshwater cements in molds ($\delta^{18}\text{O}$ of −2‰ to +1‰, PDB) from the late calcite cements ($\delta^{18}\text{O}$ of −6‰ to −3‰, PDB). Late calcite cements may have been derived from pressure

solution at stylolites. Diagenetic chert, saddle dolomite, and quartz are likely products of hydrothermal alteration. Relatively intense diagenetic alteration in synrift carbonates (compared with the sag) might be resulting from repeated influxes of reactive freshwater during shallow and moderate burial. The synrift is also at slightly greater depths than the sag interval, which may have caused increased pressure solution (stylolites) and cementation during deep burial.

DEPOSITIONAL SYSTEMS IN THE SAG INTERVAL

The sag interval is the upper part of the presalt in the Kwanza Basin and is generally overlain by evaporites of the Loeme Salt. The sag interval extends over most structural highs and thickens off structure (Figure 4). The sag is lower to lower upper Aptian and includes the upper part of ostracod zone A10 as well as AS11 and AS12 from Bate (1999). The sag can be further divided into a lower sag interval (AS10–AS11) and an upper sag interval (AS11–AS12). Bate (1999) interpreted deposition in this area and during this time period to be dominated by saline lakes. Our depositional facies and stable isotope compositions support that interpretation. The $\delta^{18}\text{O}$ compositions of carbonate phases in the sag are generally heavier (higher $\delta^{18}\text{O}$) than the synrift (Figure 16), which supports deposition in more evaporated water in the sag (Gat, 1996). The higher $\delta^{13}\text{C}$ values in the sag also indicate deposition in more evaporated lake waters than the synrift (Talbot, 1990).

Distinct mounds identified from seismic data (Figure 17A) occur in isolated buildups, but they can also be identified along the margins of depositional platforms. Isolated mound buildups are found primarily in the lower sag and have lithologies and depositional facies that are very different from platform facies; however, both pass laterally off structure into deeper-water, more organic-rich facies (similar to modern Lake Tanganyika; Cohen and Thouin, 1987; Cohen, 1989; Scholz et al., 2003). Seismic data also show platforms in the sag interval (Figure 17B).

Isolated Buildups

Isolated buildups formed on paleohighs during deposition of the “lower sag” interval (Figure 4). Large,

isolated buildups contain smaller internal mounds that are commonly 100–200 m (328–656 ft) thick and 1–2 km (0.6–1.2 mi) across (Figure 17A). The main facies in the isolated buildups is microbial chert boundstone with thick branches, pillars, and domal morphologies and internal, growth-related cavities (Figures 4, 8, 9). Other lithologies and facies in the isolated buildups include (1) dolomites (some replacive wackestone–packstones and grainstones and some primary precipitates, including dolomitic microbialites), (2) limestones with fibrous shrubby growth structures and grainstones containing spherulites and intraclasts, and (3) coarse packstones and grainstones with clasts of chert (lithoclast breccias).

Carbonate Platforms

Lacustrine carbonate platforms developed on broad structural highs during deposition of the sag interval (Figure 4). Lacustrine platforms are up to 20–50 km (12–31 mi) long, 10–20 km (6–12 mi) wide, and 200–350 m (656–1148 ft) thick, and they are seismically mappable (Figure 17B). The “building blocks” of these platforms are carbonate grains and reefal organisms that are very different from marine carbonates. Shrubby microbial boundstones are the main reefal material identified in sag platforms, but spherulites and intraclasts are also major carbonate grains. Shrubby boundstones and spherulite–intraclast grainstones are important reservoir facies in the middle of the platforms and decrease off structure (Figure 4). Wackestones and packstones with calcareous grains and intergranular dolomite occur as interbeds on the crest of the platforms and thicken to the margins of the platforms (Figure 4). Stevensite in dolomitic or spherulitic mudstones and wackestones increases with stratigraphic depth in the sag and is also more abundant on the flanks of the platforms. Chert beds (1 cm [0.4 in.] to 200 cm [80 in.] thick) are scattered throughout the platform strata. Some chert beds contain distinct microbial structures suggesting that they are boundstones, but other chert beds were probably deposited as either fine (muddy) silica or fine (muddy) carbonate that was replaced by silica. Silicified ostracods are present in many cherts, but ostracods are rare in most other sag carbonates. Shrubby boundstones and spherulite–intraclast grainstones generally increase in abundance upward, becoming abundant in

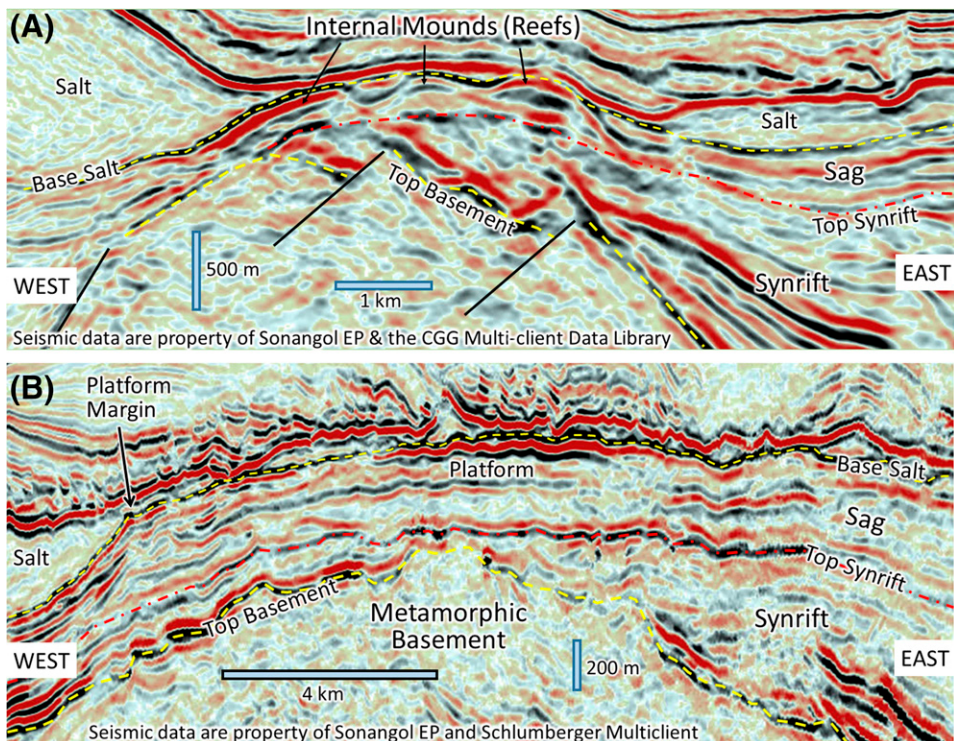


Figure 17. Prestack-depth-migrated seismic data. (A) Profile over an isolated buildup showing three internal mounds that amalgamate in three dimensions. Profile does not go through the thickest parts of the center and left mounds. Excellent reservoir occurs in microbial cherts in the internal mounds. (B) Profile over a presalt carbonate platform in the sag interval. Shubby boundstones and grainstones occur on the platform top. Figure 4 shows schematically where these lines fit on a depositional profile and link seismic with depositional facies shown on core photographs and thin-section photos.

the uppermost part of the sag in the middle of platforms (Figure 4).

Off-Structure Mud-Rich Strata

Mud-rich facies include organic-rich mudstones and stevensite with spherulites or dolomite. Both types of mud-rich rocks generally lack mollusks but contain ostracods in a few intervals. These mud-rich facies occur (1) in the lower part of the sag on platforms, (2) on the flanks of platforms, and (3) above isolated buildups in deeper areas (Figure 4).

Interpretation of Sag Depositional System

The sag interval is interpreted as deposited at various depths in highly saline and alkaline waters (Figure 4). The lack of mollusks in what appear to be relatively shallow water deposits on platforms and isolated buildups suggests that these lacustrine environments were too saline and alkaline for mollusks to thrive. This is also supported by the scarcity of ostracods except in what appear to be flooding and deepening events (similar to Wright and Barnett, 2015). The presence of stevensite clay provides additional evidence for highly

alkaline lake water ($\text{pH} > 9$; Khoury et al., 1982; Jones, 1986; Tosca and Wright, 2015).

Isolated chert-rich buildups are dominated by clotted structures characteristic of microbial deposition (Chafetz and Guidry, 1999; Guidry and Chafetz, 2003; Scholle and Ulmer-Scholle, 2003). In other locations in the basin, many cherts are replacive, but a depositional origin is indicated for these microbial cherts by depositional clasts containing chert with microbial structures and chalcedony cements that are truncated at the edges of the clasts (Figure 9F). In addition, the $\delta^{18}\text{O}$ compositions for the microbial cherts and chalcedony ($\delta^{18}\text{O}$ of 39‰–40‰, SMOW) are only compatible with precipitation at relatively cool surface temperatures (23°C–27°C [73°F–81°F]) in highly saline waters ($\delta^{18}\text{O}$ of 5‰–6‰, SMOW; Figure 10). The buildup morphology and lack of progradation suggest deposition during transgressions associated with relatively rapid lake level rises. These isolated buildups are located west (basinward) of the upper sag lacustrine platforms and are structurally deeper than platforms (Figure 4). The Pleistocene and Holocene buildups at Pyramid Lake, northwest Nevada (Benson, 1994, 2004; Della Porta, 2015) are good morphologic analogs for these buildups, but they are calcitic, rather than chert dominated. A marked change in facies from microbial

chert boundstones up to organic-rich or stevensite-rich muds suggests a rapid deepening in the upper sag. That lake level rise caused carbonate deposition to shift to paleohighs to the east, resulting in carbonate platforms developed along the Atlantic hinge line (Figure 4).

Marls with stevensite, spherulites, and dolomite generally appear to be deposited in shallower water than organic-rich muds, but lake circulation and chemistry (oxidation and alkalinity) independent of depth are also factors in variations between organic-rich muds and stevensite-rich marls. Stevensite requires very high alkalinity, but that high alkalinity could extend from substantial water depths to shallow oxidized waters. Deposition of organic-rich muds requires anoxic conditions that are common in deep water and could not occur in shallow, oxidized waters.

Sag platforms have distinct lateral and vertical facies patterns (Figure 4). In the middle of the platforms, spherulite wackestones and packstones in the lower sag pass upward to intraclast-spherulite packstone-grainstones and shrubby boundstones, indicating a general shallowing during deposition of the upper sag. The widespread occurrence of shrubby boundstones and intraclast-spherulite packstone-grainstones in the middle of the platforms (Figure 4) suggests that shallow, relatively high-energy environments were widespread, resulting in widespread stratified porosity and permeability on the platform top.

DEPOSITIONAL SYSTEMS IN THE UPPER SYNRIFT INTERVAL

The upper synrift in the Kwanza Basin can be divided into three general areas: (1) eastern, siliciclastic rich; (2) central, platform; and (3) western, basinward (Figure 4).

Eastern, Siliciclastic-Rich Area

The eastern Kwanza Basin contains an upper synrift section that is characterized by conglomerate and coarse sandstone, shelly conglomerate and sandstone, and green fine sandstone and siltstone facies (Figure 4). Mollusk-rich limestones and dolomites are also present in some intervals. In general, mollusk-rich

carbonates increase and coarse sandstones and conglomerates decrease to the west. The lower synrift contains mollusk packstones and grainstones with interbeds of organic-rich mudstones along the flanks of half grabens in eastern parts of the Kwanza Basin.

Central, Platform Area

The central Kwanza Basin contains a lower synrift (middle to lower Barremian) section that is generally confined to presalt half grabens and an upper synrift section that had deposition extending over structural highs (Figure 4). The centers of half grabens are expected to be organic-rich muds, similar to the Bucamazi Formation (Hauterivian–Aptian) of northern Angola (Schoellkopf and Patterson, 2000).

On structural highs, the upper synrift is dominated by mollusk grainstones (coquinas) and mollusk wackstone–packstones (Figure 4). Packstones and grainstones are dominant at the top of the synrift and common throughout the upper synrift on depositional highs. Ostracod-rich zones occur sporadically in the middle and lower part of the upper synrift. The top of the upper synrift has a sharp contact with overlying mud-rich units. Vuggy, dissolution-related porosity is common at the top of the synrift. Seismic data show the lowest sag strata onlapping the top of synrift on structural highs.

Western, Basinward Area

The synrift section in the western Kwanza Basin contains various lithologies and facies. On structural highs, thin mollusk wackestones, packstones, and grainstones are interbedded with several facies, including lime mudstones, ostracod wackestones, organic-rich carbonate mudstones, siliceous mudstones, and dolomites. Our wells do not penetrate synrift half grabens in axial positions, but we infer these areas to be dominated by organic-rich mudstones.

Interpretation

The upper synrift is characterized by mollusk shells and fragments (coquinas) in contrast to the sag interval, which is largely devoid of mollusk fragments. This suggests that the upper synrift was deposited in relatively freshwater lakes with mollusk packstones

and grainstones on the depositional highs and organic-rich mudstones in depositional lows, similar to Lake Tanganyika (Cohen and Thouin, 1987; Cohen, 1989; Scholz et al., 2003). Stable isotopic compositions of upper synrift limestones (Figure 16) are consistent with deposition in relatively fresh-to-moderately evaporated lake water (Talbot, 1990).

The upper synrift interval is similar to the Toca T3 (upper Barremian) interval in the Lower Congo Basin of northern Angola and Republic of Congo (Harris, 2000). This interval also corresponds to the presalt Phases 5-6 (AS9–AS10) of Bate (1999), which are interpreted as a time of relatively fresh-to-moderately saline lakes. Mollusk grainstones preferentially accumulated in shallow lake environments with at least occasional currents. Interbedding of mollusk grainstones and deep-water organic mudstones in parts of the basin in the upper Barremian suggests rapid, high-amplitude lake level rises and falls, similar to those observed at the Great Salt Lake during the last 15,000 yr (Eardley et al., 1957).

Several features suggest a significant unconformity at the top of the synrift: (1) a sharp lithology change from mollusk-rich limestones up to organic-rich mudstones; (2) seismic onlap onto the upper synrift surface, which is characteristic of sequence boundaries (unconformities; Vail, 1987; Van Wagoner et al., 1988); (3) vuggy porosity immediately below the top synrift, likely formed by karst-related dissolution; (4) early calcite cements that have crystal morphologies similar to freshwater cements (Longman, 1980); and (5) isotope compositions of calcite cements similar to low-temperature meteoric cements (Figure 16).

RESERVOIR CHARACTERISTICS

Presalt wells producing from the sag interval in Brazil have had impressive flow rates, with production of more than 25,000 barrels of oil per well per day for several years (PreSalt.com, 2015). Flow tests from the Kwanza Basin have also been impressive, with rates of more than 5000 BOE per day in tests limited by surface facilities (Cobalt International Energy, 2012, 2013, 2014). The best reservoir facies in the upper sag platforms in the Kwanza Basin are generally shrubby microbial boundstones and intraclastic grainstones. Shrubby boundstones have high permeabilities associated with their primary pores between shrub

branches (Figures 5–7). Those pores are elongate (almost planar) and have pore throats that are similar in width to the rest of the pore network. Microbial cherts are the dominant reservoir facies in the isolated buildups. Vugs and fractures are common in microbial cherts (Figures 8 and 9) and directly relate to the high permeabilities observed in well tests. Spherulitic wackestones and packstones often have moderate-to-poor porosity and low permeability, but have a high enough porosity and permeability to be considered pay in some intervals.

Mollusk packstones and grainstones (coquinas) are the main reservoir facies in the upper synrift interval. The effective porosity in mollusk packstones and grainstones (coquinas) is controlled by diagenesis. In grainstones, porosity is primarily found where intergranular cements are minimal (Figure 15B, C). In some intervals, mollusks were preferentially dissolved, creating moldic porosity (Figure 14A). Early dissolution associated with freshwater and late dissolution associated with hydrothermal fluids have resulted in connected vugs in some intervals. Other parts of the synrift contain porosity associated with dolomitization, silicification and associated fractures, or partial silicification and preserved intergranular or moldic porosity (Figure 15B, G).

DISCUSSION

Many geological controversies have emerged from studies of the presalt of the South Atlantic (Wright and Barnett, 2015), and our data have a bearing on six of these discussions: (1) similarities of Kwanza Basin presalt to Brazil presalt, (2) influence of marine water, (3) origin of the shrubby facies—microbial or abiotic—and relation to travertines, (4) origin of spherulites and association with stevensite and porosity, (5) original mineralogy and possible recrystallization of shrubs and spherulites, and (6) origin of cherts—depositional or diagenetic.

Similarities of Kwanza Basin Presalt to Brazil Presalt

Little has been published on the presalt in the current deep-water part of Brazil; however, bits that have been published make the Brazilian presalt appear similar to what is observed in the Kwanza Basin. As

Quirk et al. (2013) show, the Kwanza Basin was adjacent to the Campos Basin, offshore Brazil, during the early stages of rifting. Carminatti et al. (2008) show carbonate platforms in Brazil that are similar to carbonate platforms that we observe in the sag (Figures 4 and 17B). We suspect that the “clean microbialite (reservoirs)” described by Carminatti et al. (2008) immediately below salt are similar to our shrubby boundstone facies and may also include grainstone facies that we observe on Kwanza platforms. Descriptions of shrubby facies by Wright and Barnett (2015) in rocks inferred to be in the Tupi (Lula) field area are similar to ours. Carminatti et al. (2008) describe coquinas deeper in the section, similar to the synrift in the Kwanza Basin.

Influence of Marine Water

Similar to Wright and Barnett (2015), we did not recognize any distinctly marine fossils in the presalt. Interestingly, planktonic foraminifera were in places observed from cuttings in the presalt interval; however, those foraminifera were dated as Albian, indicating contamination of the cuttings, not foraminifera in the presalt. An unconformity at the top of the presalt carbonate is overlain by interbedded dolomites and anhydrites, with anhydrites becoming more abundant and massive upward until the section passes into halite. The interbedded dolomite and anhydrite succession is probably part of the initial marine transgression that also deposited the Loeme salt.

Origin of the Shrubby Facies—Microbial or Abiotic—and Relation to Travertines

Arguments have been made by Dorobek et al. (2012) and Wright and Barnett (2015) that the shrubby facies of Brazil is largely abiotic. A major argument for an abiotic origin is the common fibrous nature of crystals in the shrubs that suggests rapid precipitation similar to some travertines and marine cements (Wright and Barnett, 2015). Although the shrubs observed in the Angola presalt commonly have fibrous-to-prismatic crystals, those crystals generally have an upward orientation and growth pattern (Figure 5). Vertically elongate vugs generally remain open adjacent to fibrous bundles of calcite crystals, suggesting that the fibrous-to-prismatic crystals in the shrubs are not

simple pore-filling cement; otherwise, they would have also filled the adjacent pores. Botryoids of fibrous calcite cement crystals similar to marine cements occur in a few locations (Figure 13C), but they are distinctly different from most shrubby boundstones. Micritization and erosion embayments in the shrubs suggest alteration and local erosion by microbes (Figures 5B; 7A–C). A microbial mat or biofilm at the top of the shrubby growth might not have been the cause of the calcareous precipitate, but it could have prevented sediment from falling between the shrub branches and could have prevented or at least slowed supersaturated waters from percolating down and precipitating cements between the branches.

Even within the width of a core, shrubs and domal microbial growths show differential vertical growth and the ability to create depositional highs (Figures 5A; 6A, B), similar to modern coral and coralline algal reefs. This preferential vertical growth toward sunlight would be consistent with photosynthetic microbial organisms. This type of vertical growth may have allowed microbial growths to build upon each other and perpetuate as depositional highs.

Although some of the shrubby fabrics resemble travertine, most of the shrubby facies studied in the Kwanza Basin are not interpreted as travertine. We agree with the eloquent reasoning of Wright and Barnett (2015) on this subject. Several other features do not support a travertine origin: (1) stable oxygen isotope analyses are consistent with low temperature, not high temperature, precipitation; (2) the porosity interval that includes the shrubby facies has seismic attributes that extend over an area that is approximately 8 km (5 mi) long and 5 km (3 mi) wide in the middle of the platform; and (3) shrubby facies are repeatedly interbedded with normal lacustrine facies, including spherulitic wackestone–packstone, mudstones, and intraclastic grainstones with intraclasts of shrubby facies, suggesting that the shrubby facies is a normal, repeated, lacustrine depositional facies.

Origin of Spherulites and Association with Stevensite and Porosity

Spherulites are common in both the Brazil and the Angola presalt sag interval. Spherulites have been

interpreted as forming by displacive growth in the very shallow subsurface (Dorobek et al., 2012; Wright and Barnett, 2015). Wright and Barnett (2015) also reason that the waters in Brazil lakes were highly alkaline, which is consistent with the highly alkaline waters interpreted for Kwanza sag environments. The lack of calcitic, micritic mud in the presence of spherulites is striking. Magnesium-silicate gels have been suggested as a critical factor in spherulite precipitation (Tosca and Wright, 2015; Wright and Barnett, 2015). Where spherulites occur with stevensite, it is logical to interpret Mg-silicate gels as a factor associated with spherulite precipitation. However, in many other locations, spherulites are not associated with stevensite, and hence we interpret spherulite precipitation as occurring in other types of lake-bottom sediment and possibly even microbial gels. In all cases, the lake-bottom waters were supersaturated with respect to calcite.

Original Mineralogy and Possible Recrystallization of Shrubs and Spherulites

We agree with Wright and Barnett (2015) that the original mineralogy of most of the shrubs and spherulites was probably calcite. Cathodoluminescence patterns suggest some recrystallization in shrubby facies and spherulites, but prismatic crystals parallel original fibrous crystals and tend to not cut across the original crystal fabric (Figures 7F). Mollusks in the synrift show calcitization (neomorphism) of aragonite, similar to that observed in marine carbonates, but very different from calcite crystal fabrics in shrubs and spherulites. Equant calcite crystals commonly cut across original crystal fabrics in calcitized aragonites in mollusk shells (Figure 15C, E). Many calcite crystals in shrubs and spherulites are still fibrous, whereas others are prismatic to wedge shaped, but the margins of the prismatic and wedge-shaped crystals still follow the original radiating fabric in spherulites and are vertically oriented growth fabrics in shrubs (Figures 7D and 12). Spherulites and shrub calcite have high strontium concentrations (average strontium concentration of 3000 ppm). Although these are elevated similar to neomorphosed marine aragonite, we explain these as related to generally high strontium concentrations in the highly saline and alkaline lake water.

Origin of Cherts—Depositional or Diagenetic

Cherts are a major reservoir facies in isolated buildups on basinward structures in the Kwanza Basin (Figure 4) and appear to be the result of silica precipitation at low temperatures associated with microbial growths. We have not found close analogs in other locations. Silica precipitation in hydrothermal sinters associated with microbes has been widely documented and is in some ways similar (Braunstein and Lowe, 2001; Guidry and Chafetz, 2003). Clasts with truncated chalcedony cements in the presalt indicate that silica was precipitated during reef-like deposition. The very high $\delta^{18}\text{O}$ values of the microbial cherts and chalcedonies indicate deposition in highly evaporated waters at relatively low temperatures. Seismic data indicate that these microbial cherts occur as buildups 200 m (656 ft) thick and 1–2 km (0.6–1.2 mi) across, and they are not associated with faults or any apparent conduits for hydrothermal waters. As Wright and Barnett (2015) note, the presalt sag lake waters were very alkaline, with high concentrations of dissolved silica. In other parts of the basin, vertical seismic discontinuities (pipes and planes) suggest deep-seated conduits for hydrothermal fluids. Hydrothermal fluids would have passed through substantial amounts of volcanic material, which could have contributed silica that was ultimately piped into the sag lake (or lakes); however, we do not see evidence for hydrothermal vents being directly responsible for the large microbial mounds in basinward parts of the Kwanza Basin.

CONCLUSIONS

Lacustrine sedimentation has resulted in many unusual carbonate and chert facies in the presalt of the Kwanza Basin. The upper synrift is dominated by mollusk packstones and grainstones (coquinas) deposited in the shallow part of relatively fresh lakes. Organic-rich mudstones were deposited in deeper water adjacent to depositional highs in both the upper synrift and sag. Sag deposition occurred in highly evaporated, highly alkaline lake water. Shrubby microbial boundstones and intraclastic grainstones were deposited in shallow, moderate- to high-energy water on broad lacustrine platforms during deposition of the sag interval (Figure 4). Wackestones and packstones with calcitic spherulites in a dolomitic to argillaceous

matrix were deposited in slightly deeper lake water on the flanks of the structures and on top of the structures during intraformational transgressions. Microbial chert boundstones formed buildups on isolated structural highs basinward of the sag platforms (Figure 4).

An excellent petroleum system exists in the presalt in the Kwanza Basin. After substantial burial, oil and gas were generated from organic-rich muds deposited in presalt lows. Oil generation probably started in the deeper parts of synrift grabens during and shortly after upper sag deposition. Generation of oil probably continues to the present in organic-rich parts of the sag. Excellent reservoir facies (shrubby microbial boundstones, intraclast grainstones, and microbial cherts) developed on carbonate platforms and on isolated highs basinward of the platforms. The Loeme salt was deposited over the presalt interval, giving an excellent vertical seal to hydrocarbons maturing below and causing oil and gas to be trapped in reservoir rocks in the uppermost presalt.

REFERENCES CITED

- Al Rajaibi, I. M., C. Hollis, and J. H. MacQuaker, 2015, Origin and variability of a terminal Proterozoic primary silica precipitate, Athel Siliclyte, South Oman Salt Basin, Sultanate of Oman: *Sedimentology*, v. 62, p. 793–825, doi:[10.1111/sed.12173](https://doi.org/10.1111/sed.12173).
- Bate, R. H., 1999, Non-marine ostracod assemblages of the pre-salt rift basins of West Africa and their role in sequence stratigraphy, in N. R. Cameron, R. H. Bate, and V. S. Clure, eds., *The oil and gas habitats of the South Atlantic*: Geological Society, London, Special Publications 1999, v. 153, p. 283–292, doi:[10.1144/GSL.SP.1999.153.01.17](https://doi.org/10.1144/GSL.SP.1999.153.01.17).
- Behr, H.-J., 2002, Magadiite and Magadi chert: A critical analysis of the silica sediments in Lake Magadi, Kenya, in R. W. Remaut and G. M. Ashley, eds., *Sedimentation in continental rifts*: SEPM Special Publication 73, p. 257–273, doi:[10.2110/pec.02.73.0257](https://doi.org/10.2110/pec.02.73.0257).
- Benson, L. V., 1994, Carbonate deposition, Pyramid Lake subbasin, Nevada: 1. Sequence of formation and elevational distribution of carbonate deposits (tufas): *Palaeogeography, Palaeoclimatology, Palaeoecology*, v. 109, p. 55–87, doi:[10.1016/0031-0182\(94\)90118-X](https://doi.org/10.1016/0031-0182(94)90118-X).
- Benson, L. V., 2004, The tufas of Pyramid Lake, Nevada: US Geological Survey Circular 1267, 14 p.
- Braunstein, D., and D. R. Lowe, 2001, Relationship between spring and geyser activity and the deposition and morphology of high temperature (>73°C) siliceous sinter, Yellowstone National Park, Wyoming, U.S.A.: *Journal of Sedimentary Research*, v. 71, p. 747–763, doi:[10.1306/2DC40965-0E47-11D7-8643000102C1865D](https://doi.org/10.1306/2DC40965-0E47-11D7-8643000102C1865D).
- Carminatti, M., B. Wolff, and L. Gamboa, 2008, New exploratory frontiers in Brazil: Proceedings of the 19th World Petroleum Congress, Madrid, Spain, June 29–July 3, 2008, 11 p.
- Cazier, E. C., C. Bargas, L. Buambua, S. Cardosa, H. Ferreira, A. Lopez, T. Nicholson, C. Olson, A. Saller, and J. Shinol, 2014, Petroleum geology of Cameia field, deepwater pre-salt Kwanza Basin, Angola, West Africa: AAPG Search and Discovery article 20275, accessed January 9, 2015, http://www.searchanddiscovery.com/documents/2014/20275cazier/ndx_cazier.pdf.
- Cerling, T. E., 1994, Chemistry of closed basin lake waters: A comparison between African Rift Valley and some central North American rivers and lakes, in E. H. Gierlowski-Kordesch and K. Kelts, eds., *The global geological record of lake basins*: Cambridge, United Kingdom, Cambridge University Press, p. 29–30.
- Chafetz, H. S., and S. A. Guidry, 1999, Bacterial shrubs, crystal shrubs, and ray-crystal shrubs: Bacterial versus abiotic precipitation: *Sedimentary Geology*, v. 126, p. 57–74, doi:[10.1016/S0037-0738\(99\)00032-9](https://doi.org/10.1016/S0037-0738(99)00032-9).
- Cobalt International Energy, 2012, Press releases, accessed September 20, 2015, http://www.cobaltintl.com/newsroom#press_releases.
- Cobalt International Energy, 2013, Press releases, accessed September 20, 2015, http://www.cobaltintl.com/newsroom#press_releases.
- Cobalt International Energy, 2014, Press releases, accessed September 20, 2015, http://www.cobaltintl.com/newsroom#press_releases.
- Cohen, A. S., 1989, Facies relationships and sedimentation in large rift lakes and implications for hydrocarbon exploration: Examples from lakes Turkana and Tanganyika: *Palaeogeography, Palaeoclimatology, Palaeoecology*, v. 70, p. 65–80, doi:[10.1016/0031-0182\(89\)90080-1](https://doi.org/10.1016/0031-0182(89)90080-1).
- Cohen, A. S., and C. Thouin, 1987, Nearshore carbonate deposits in Lake Tanganyika: *Geology*, v. 15, p. 414–418, doi:[10.1130/0091-7613\(1987\)15<414:NCDILT>2.0.CO;2](https://doi.org/10.1130/0091-7613(1987)15<414:NCDILT>2.0.CO;2).
- Cohen, K. M., S. C. Finney, P. L. Gibbard, and J.-X. Fan, 2013, The ICS international chronostratigraphic chart: *Episodes*, v. 36, p. 199–204.
- Dale, C. T., J. R. Lopes, and S. Abilio, 1992, Takula oil field and the greater Takula area, Cabinda, Angola: Chapter 13, in M. T. Halbouty, ed., *Giant oil and gas fields of the decade 1978–1988*: AAPG Memoir 54, p. 197–215.
- Davison, I., 2007, Geology and tectonics of the South Atlantic Brazilian salt basins, in A. C. Ries, R. W. H. Butler, and R. H. Graham, eds., *Deformation of the continental crust: The legacy of Mike Coward*: Geological Society, London, Special Publications 2007, v. 272, p. 345–359, doi:[10.1144/GSL.SP.2007.272.01.18](https://doi.org/10.1144/GSL.SP.2007.272.01.18).
- Della Porta, G., 2015, Carbonate build-ups in lacustrine, hydrothermal and fluvial settings: Comparing depositional geometry, fabric types and geochemical signature, in D. W. J. Bosence, K. A. Gibbons, D. P. Le Heron, W. A. Morgan, T. Pritchard, and B. A. Vining, eds., *Microbial carbonates in space and time: Implications for global exploration and production*: Geological Society,

- London, Special Publications 2015, v. 418, p. 17–68, doi:[10.1144/SP418.4](https://doi.org/10.1144/SP418.4).
- Dickson, J. A. D., 1966, Carbonate identification and genesis as revealed by staining: *Journal of Sedimentary Petrology*, v. 36, p. 491–505.
- Dorobek, S. I., L. Piccoli, B. Coffey, and A. Adams, 2012, Carbonate rock-forming processes in the pre-salt “sag” successions of Campos Basin, offshore Brazil: Evidence for seasonal, dominantly abiotic carbonate precipitation, substrate controls, and broader geologic implications: AAPG Hedberg Conference: Microbial Carbonate Reservoir Characterization, Houston, Texas, June 4–8, 2012, AAPG Search and Discovery article 90153, accessed September 7, 2015, http://www.searchanddiscovery.com/pdfz/abstracts/pdf/2012/90153hedberg/abstracts/ndx_dorobek.pdf.html.
- Eardley, A. J., 1938, Sediments of Great Salt Lake, Utah: AAPG Bulletin, v. 22, no. 10, p. 1305–1411.
- Eardley, A. J., V. Gvоздetsky, and R. E. Marsell, 1957, Hydrology of Lake Bonneville and sediments and soils of its basin: *Geological Society of America Bulletin*, v. 68, p. 1141–1201, doi:[10.1130/0016-7606\(1957\)68\[1141:HOLBAS\]2.0.CO;2](https://doi.org/10.1130/0016-7606(1957)68[1141:HOLBAS]2.0.CO;2).
- Fairhead, J. D., and W. Wilson, 2005, Plate tectonic processes in the South Atlantic Ocean: Do we need deep mantle plumes? in G. R. Fouger, J. H. Natland, D. C. Presnall, and D. L. Anderson, eds., Plates, plumes, and paradigms: *Geological Society of America Special Paper* 388, p. 537–553, doi:[10.1130/0-8137-2388-4.537](https://doi.org/10.1130/0-8137-2388-4.537).
- Flügel, E., 1982, Microfacies analysis of limestones: New York, Springer-Verlag, 633 p., doi:[10.1007/978-3-642-68423-4](https://doi.org/10.1007/978-3-642-68423-4).
- Friedman, I., and J. R. O’Neil, 1977, Compilation of stable isotope fractionation factors of geochemical interest: US Geological Survey Professional Paper 440-K, 12 p.
- Gat, J. R., 1996, Oxygen and hydrogen isotopes in the hydrologic cycle: *Annual Review of Earth and Planetary Sciences*, v. 24, p. 225–262, doi:[10.1146/annurev.earth.24.1.225](https://doi.org/10.1146/annurev.earth.24.1.225).
- Greenhalgh, J., R. Borsato, F. Mathew, G. Duncan-Jones, I. Pimenta, J. Marques da Silva, and L. Narciso da Silva, 2012, Petroleum plays and prospectivity in the Kwanza and Benguela Basins of offshore Angola: AAPG Search and Discovery article 10443, accessed January 14, 2014, http://www.searchanddiscovery.com/documents/2012/10443greenhalgh/ndx_greenhalgh.pdf.
- Guardado, L. R., L. A. P. Gamboa, and C. F. Lucchesi, 1990, Petroleum geology of the Campos Basin, Brazil: A model for a producing Atlantic-type basin, in J. D. Edwards and P. A. Santogrossi, eds., Divergent-passive margin basins: AAPG Memoir 48, p. 3–80.
- Guidry, S. A., and H. S. Chafetz, 2003, Anatomy of siliceous hot springs: Examples from Yellowstone National Park, Wyoming, USA: *Sedimentary Geology*, v. 157, p. 71–106, doi:[10.1016/S0037-0738\(02\)00195-1](https://doi.org/10.1016/S0037-0738(02)00195-1).
- Harris, N. B., 2000, Toca carbonate, Congo Basin: Response to an evolving rift lake, in M. R. Mello and B. J. Katz, eds., Petroleum systems of South Atlantic margins: AAPG Memoir 73, p. 341–360.
- Jones, B. F., 1986, Clay mineral diagenesis in lacustrine settings, in F. A. Mumpton, ed., *Studies in diagenesis: US Geological Survey Bulletin* 1578, p. 291–300.
- Khoury, H. N., D. D. Eberl, and B. F. Jones, 1982, Origin of magnesium clays from the Armargosa Desert, Nevada: *Clays and Clay Minerals*, v. 30, p. 327–336, doi:[10.1346/CCMN.1982.0300502](https://doi.org/10.1346/CCMN.1982.0300502).
- Land, L. S., 1985, The origin of massive dolomite: *Journal of Geological Education*, v. 33, p. 112–125.
- Laval, B., S. L. Cady, J. C. Pollack, C. P. McKay, J. S. Bird, J. P. Grotzinger, D. C. Ford, and H. R. Bohm, 2000, Modern freshwater microbialite analogues for ancient dendritic reef structures: *Nature*, v. 407, p. 626–629, doi:[10.1038/35036579](https://doi.org/10.1038/35036579).
- Ligang, Z., L. Jingxiu, Z. Huanbo, and C. Zhensheng, 1989, Oxygen fractionation in the quartz-water-salt system: *Economic Geology and the Bulletin of the Society of Economic Geologists*, v. 84, p. 1643–1650, doi:[10.2113/gsecongeo.84.6.1643](https://doi.org/10.2113/gsecongeo.84.6.1643).
- Longman, M. W., 1980, Carbonate diagenetic textures from nearsurface diagenetic environments: AAPG Bulletin, v. 64, no. 4, p. 461–487.
- McHargue, T. R., 1990, Stratigraphic development of proto-South Atlantic rifting in Cabinda, Angola—A petrolierous lake basin, in B. J. Katz, ed., *Lacustrine basin exploration: Case studies and modern analogs*: AAPG Memoir 50, p. 307–326.
- O’Neil, J. R., and R. L. Hay, 1973, $^{18}\text{O}/^{16}\text{O}$ ratios in cherts associated with the saline lake deposits of east Africa: *Earth and Planetary Science Letters*, v. 19, p. 257–266, doi:[10.1016/0012-821X\(73\)90126-X](https://doi.org/10.1016/0012-821X(73)90126-X).
- Poropat, S. F., and J.-P. Colin, 2012, Early Cretaceous ostracod biostratigraphy of eastern Brazil and western Africa: An overview: *Gondwana Research*, v. 22, p. 772–798, doi:[10.1016/j.gr.2012.06.002](https://doi.org/10.1016/j.gr.2012.06.002).
- PreSalt.com, 2015, Production by well, accessed September 20, 2015, <http://www.presalt.com/en/pre-salt-production/brazilian-pre-salt-production-by-well/>.
- Quirk, D. G., M. Hertle, J. W. Jeppesen, M. Raven, W. U. Mohriak, D. J. Kann, M. Nørgaard, et al., 2013, Rifting, subsidence and continental break-up above a mantle plume in the central South Atlantic, in W. U. Mohriak, A. Danforth, P. J. Post, D. E. Brown, G. C. Tari, M. Nemčok, and S. T. Sinha, eds., *Conjugate divergent margins*: Geological Society, London, Special Publications 2013, v. 369, p. 185–214, doi:[10.1144/SP369.20](https://doi.org/10.1144/SP369.20).
- Saller, A. H., 1992, Calcitization of aragonite in Pleistocene limestones of Enewetak Atoll, Bahamas, and Yucatan—An alternative to thin-film neomorphism: *Carbonates and Evaporites*, v. 7, p. 56–73, doi:[10.1007/BF03175393](https://doi.org/10.1007/BF03175393).
- Schoellkopf, N. B., and B. A. Patterson, 2000, Petroleum systems of offshore, Cabinda, Angola, in M. R. Mello and B. J. Katz, eds., *Petroleum systems of South Atlantic margins*: AAPG Memoir 73, p. 361–376.
- Scholle, P. A., and D. Ulmer-Scholle, 2003, A color guide to the petrography of carbonate rocks: Grains, textures, porosity, diagenesis: AAPG Memoir 77, 474 p.

- Scholz, C. A., J. W. King, G. S. Ellis, and P. K. Swart, 2003, Paleolimnology of Lake Tanganyika, East Africa over the past 100 kyr: *Journal of Paleolimnology*, v. 30, p. 139–150, doi:[10.1023/A:1025522116249](https://doi.org/10.1023/A:1025522116249).
- Shanks, W. C. III, J. C. Alt, and L. A. Morgan, 2007, Geochemistry of sublacustrine hydrothermal deposits in Yellowstone Lake—Hydrothermal reactions, stable-isotope systematics, sinter deposition, and spire formation: US Geological Survey Professional Paper 1717G, p. 205–234.
- Talbot, M. R., 1990, A review of the palaeohydrological interpretation of carbon and oxygen isotopic ratios in primary lacustrine carbonates: *Chemical Geology: Isotope Geoscience Section*, v. 80, p. 261–279, doi:[10.1016/0168-9622\(90\)90009-2](https://doi.org/10.1016/0168-9622(90)90009-2).
- Thompson, D. L., J. D. Stilwell, and M. Hall, 2015, Lacustrine carbonate reservoirs from Early Cretaceous rift lakes of Western Gondwana: Pre-salt coquinas of Brazil and West Africa: *Gondwana Research*, v. 28, p. 26–51, doi:[10.1016/j.gr.2014.12.005](https://doi.org/10.1016/j.gr.2014.12.005).
- Torsvik, T. H., S. Rousse, C. Labails, and M. A. Smethurst, 2009, A new scheme for the opening of the South Atlantic Ocean and the dissection of an Aptian salt basin: *Geophysical Journal International*, v. 177, p. 1315–1333, doi:[10.1111/j.1365-246X.2009.04137.x](https://doi.org/10.1111/j.1365-246X.2009.04137.x).
- Tosca, N. J., and V. P. Wright, 2015, Diagenetic pathways linked to labile Mg-clays in lacustrine carbonate reservoirs: A model for the origin of secondary porosity in the Cretaceous pre-salt Barra Velha Formation, offshore Brazil, *in* P. J. Armitage, A. R. Butcher, J. M. Churchill, A. E. Csoma, C. Hollis, R. H. Lander, J. E. Omma, and R. H. Worden, eds., *Reservoir quality of clastic and carbonate rocks: Analysis, modelling and prediction*: Geological Society, London, Special Publications 2015, v. 435, doi:[10.1144/SP435.1](https://doi.org/10.1144/SP435.1).
- Vail, P. R., 1987, Seismic stratigraphy interpretation using sequence stratigraphy. Part 1: Seismic stratigraphy interpretation procedure, *in* A. W. Bally, ed., *Atlas of seismic stratigraphy: AAPG Studies in Geology* 27, p. 1–10.
- Van Damme, D., and A. Gautier, 2013, Lacustrine mollusc radiations in the Lake Malawi Basin: Experiments in a natural laboratory for evolution: *Biogeosciences*, v. 10, p. 5767–5778, doi:[10.5194/bg-10-5767-2013](https://doi.org/10.5194/bg-10-5767-2013).
- Van Wagoner, J. C., H. W. Posamentier, R. M. Mitchum, P. R. Vail, J. F. Sarg, T. S. Loutit, and J. Hardenbol, 1988, An overview of the fundamentals of sequence stratigraphy and key definitions, *in* C. K. Wilgus, B. S. Hastings, C. G. St. C. Kendall, H. W. Posamentier, C. A. Ross, and J. C. Van Wagoner, eds., *Sea-level changes: An integrated approach*: Tulsa, Oklahoma, SEPM Special Publication 42, p. 39–45, doi:[10.2110/pec.88.01.0039](https://doi.org/10.2110/pec.88.01.0039).
- Vasconcelos, C., and J. A. McKenzie, 1997, Microbial mediation of modern dolomite precipitation and diagenesis under anoxic conditions (Lagoa Vermelha, Rio de Janeiro, Brazil): *Journal of Sedimentary Research*, v. 67, p. 378–390.
- Vasconcelos, C., J. A. McKenzie, S. Bernasconi, D. Grujic, and A. J. Tien, 1995, Microbial mediation as a possible mechanism for natural dolomite formation at low temperatures: *Nature*, v. 377, p. 220–222, doi:[10.1038/377220a](https://doi.org/10.1038/377220a).
- Wright, V. P., 2012, Lacustrine carbonates in rift settings: The interaction of volcanic and microbial processes on carbonate deposition, *in* J. Garland, J. E. Neilson, S. E. Laubach, and K. J. Whidden, eds., *Advances in carbonate exploration and reservoir analysis: Geological Society, London, Special Publications* 2012, v. 370, p. 39–47, doi:[10.1144/SP370.2](https://doi.org/10.1144/SP370.2).
- Wright, V. P., and A. J. Barnett, 2015, An abiotic model for development of textures in some South Atlantic early Cretaceous lacustrine carbonates, *in* D. W. J. Bosence, K. A. Gibbons, D. P. Le Heron, W. A. Morgan, T. Pritchard, and B. A. Vining, eds., *Microbial carbonates in space and time: Implications for global exploration and production*: Geological Society, London, Special Publications 2015, v. 418, p. 209–219, doi:[10.1144/SP418.3](https://doi.org/10.1144/SP418.3).